26 Banchereau J, Steinman RM. Dendritic cells and the control of immunity. *Nature* 1998; **392**: 245–52.
27 Santini SM, Lapenta C, Logozzi M *et al.* Type I interferon as a powerful adjuvant for monocyte-derived dendritic cell development and activity *in vitro* and in Hu-PBL-SCID mice. *J Exp Med* 2000; **191**: 1777–88.
28 Cella M, Sallusto F, Lanzavecchia A. Origin, maturation and antigen presenting function of dendritic cells. *Curr Opin Immunol* 1997; **9**: 10–6.
29 Jaffe HA, Danel C, Longenecker G *et al.* Adenovirus-mediated *in vivo* gene transfer and expression in normal rat liver. *Nat Genet* 1992; **1**: 372–8.
30 Cristiano RJ, Smith LC, Kay MA, Brinkley BR, Woo SL. Hepatic gene therapy: efficient gene delivery and expression in primary hepatocytes utilizing a conjugated adenovirus-DNA complex. *Proc Natl Acad Sci USA* 1993; **90**: 11548–52.
31 Suzuki K, Aoki K, Ohnami S *et al.* Adenovirus-mediated gene transfer of interferon alpha improves dimethylnitrosamine-induced liver cirrhosis in rat model. *Gene Ther* 2003; **10**: 765–73.
32 Taguchi T. Clinical studies of recombinant interferon alfa-2a (Roferon-A) in cancer patients. *Cancer* 1986; **57**: 1705–8.

doi: 10.1111/j.1349-7006.2010.01578.x

MOLECULAR AND CELLULAR BIOLOGY, Apr. 2011, p. 1624–1636 Vol. 31, No. 8
0270-7306/11/$12.00 doi:10.1128/MCB.00470-10

Identification of *PITX1* as a *TERT* Suppressor Gene Located on Human Chromosome 5[▽]

Dong-Lai Qi,[1]† Takahito Ohhira,[1]† Chikako Fujisaki,[1] Toshiaki Inoue,[2] Tsutomu Ohta,[3] Mitsuhiko Osaki,[1] Eriko Ohshiro,[1] Tomomi Seko,[1] Shinsuke Aoki,[1] Mitsuo Oshimura,[1,4] and Hiroyuki Kugoh[1,4]*

Department of Biomedical Science, Graduate School of Medical Science, Tottori University, 86 Nishicho, Yonago 683-8503, Japan[1]; Division of Human Genome Science, Department of Molecular and Cellular Biology, School of Life Sciences, Faculty of Medicine, Tottori University, 86 Nishicho, Yonago 683-8503, Japan[2]; Center for Medical Genomics, National Cancer Center Research Institute, Tsukiji 5-1-1, Chuo-ku, Tokyo 104-0045, Japan[3]; and Chromosome Engineering Research Center, Tottori University, 86 Nishicho, Yonago 683-8503, Japan[4]

Received 19 April 2010/Returned for modification 3 June 2010/Accepted 26 January 2011

Telomerase, a ribonucleoprotein enzyme that maintains telomere length, is crucial for cellular immortalization and cancer progression. Telomerase activity is attributed primarily to the expression of telomerase reverse transcriptase (*TERT*). Using microcell-mediated chromosome transfer (MMCT) into the mouse melanoma cell line B16F10, we previously found that human chromosome 5 carries a gene, or genes, that can negatively regulate *TERT* expression (H. Kugoh, K. Shigenami, K. Funaki, J. Barrett, and M. Oshimura, Genes Chromosome Cancer 36:37–47, 2003). To identify the gene responsible for the regulation of *TERT* transcription, we performed cDNA microarray analysis using parental B16F10 cells, telomerase-negative B16F10 microcell hybrids with a human chromosome 5 (B16F10MH5), and its revertant clones (MH5R) with reactivated telomerase. Here, we report the identification of *PITX1*, whose expression leads to the downregulation of mouse *tert* (*mtert*) transcription, as a *TERT* suppressor gene. Additionally, both human *TERT* (*hTERT*) and mouse *TERT* (*mtert*) promoter activity can be suppressed by *PITX1*. We show that three and one binding site within the *hTERT* and *mtert* promoters, respectively, that express a unique conserved region are responsible for the transcriptional activation of *TERT*. Furthermore, we showed that *PITX1* binds to the *TERT* promoter both *in vitro* and *in vivo*. Thus, *PITX1* suppresses *TERT* transcription through direct binding to the *TERT* promoter, which ultimately regulates telomerase activity.

Telomeres, which are specialized chromatin structures that are located at the end of eukaryotic chromosomes, are essential for the stability and integrity of chromosomes (2). Telomere erosion results from incomplete end replication. This erosion results in the loss of about 50 to 200 bp of telomeric DNA at each cell division and eventually leads to replicative senescence (6, 18). In contrast, telomerase, the ribonucleoprotein enzyme that maintains the telomere, is active in human germ cells, stem cells, and a majority of tumors (around 90%) and immortalized cell lines but not in somatic cells, suggesting that this enzyme activity contributes to an unlimited replicative potential and neoplastic transformation. This expression profile of telomerase activity further suggests that normal human cells contain a regulatory factor(s) that suppresses telomerase activity, and that this regulation is aberrant or missing following cellular immortalization (7). The telomerase holoenzyme consists of a protein catalytic subunit telomerase reverse transcriptase (*TERT*) and an integral RNA telomerase RNA component (*TERC*). The expression of *TERT*, but not *TERC*, depends on telomerase activity. Many studies have provided evidence suggesting that ectopic *hTERT* expression into telomerase-negative normal cells, such as human fibroblasts and epithelial cells, restores telomerase activity and maintains telomeres, resulting in continuous cell division (1, 15, 16, 48). Moreover, the ectopic expression of *hTERT* in combination with activated oncogenes results in the tumorigenic conversion of normal human cells (17). These findings suggest that *TERT* is the principal component for the control of telomerase activity and is a key factor that facilitates cellular immortalization.

Microcell-mediated chromosome transfer (MMCT) is a powerful tool for (i) gene hunting, (ii) the elucidation of the essential function of products that are expressed from a specific chromosome with its endogenous physical system, and (iii) understanding the role of the components of chromosomes and understanding genome organization (12, 31). In addition, the functional analysis of cells that have undergone MMCT using a human chromosome truncated at specific sites enables the precise mapping and identification of genes involved in a particular cell function, such as telomerase regulation, during cellular aging and metastasis. This method also can be used to identify DNA repair genes whose mutation/deletion is responsible for various inherited genetic defects, to generate transgenic mice with introduced human chromosomes, and to establish animal models of human diseases (12, 31). Advances have been made in the technology of chromosome engineering using DNA targeting through homologous recombination. It has been reported that chicken pre-B DT40 cells, which are

* Corresponding author. Mailing address: Department of Biomedical Science, Graduate School of Medical Science, Tottori University, 86 Nishicho, Yonago 683-8503, Japan. Phone: 81-859-38-6412. Fax: 81-859-38-6210. E-mail: kugoh@med.tottori-u.ac.jp.
† These authors contributed equally to this work.
▽ Published ahead of print on 7 February 2011.

proficient for homologous recombination, can be used to improve the efficiency of DNA targeting (25). We and several other groups have shown that the introduction of chromosome 3, 5, 6, or 10 results in the complete repression of *hTERT* transcription in human tumor cells (10, 20, 32, 36, 37, 47). Furthermore, deletion analysis of chromosome 3 indicated three regions, 3p12-p21.1, 3p14.2-p21.1, and 3p21.3, at which *hTERT* regulatory factors might be located (10, 51). Additionally, a telomerase repressor gene(s) has been mapped to regions in 10p15.1 on chromosome 10 (32). We previously reported that the introduction of human chromosome 5 into B16F10 mouse melanoma cells inhibited the expression of *mtert*, but that late-passage clones exhibited the reactivation of telomerase activity. These results suggested that the loss of a gene(s) on this chromosome was responsible for telomerase reactivation, indicating that human chromosome 5 also contains a gene or genes that can regulate the expression of *mtert* in B16F10 cells (24). Recently, we have reported that *hTERT* has suppressed expression by the introduction of human chromosome 5 in human melanoma A2058 cells (39). Thus, these results suggested that normal human cells carry multiple telomerase repressor genes, and that these genes encode factors that regulate the activity of the enzyme.

The expression of *TERT* is accompanied by the regulation of the gene balance between positive, transcription-activating factors (c-Myc, Sp1, estrogen, and human papillomavirus E6) and negative, transcription-repressing factors (Mad1, WT1, Rb, MZF-2, CTCF, menin, transforming growth factor β [TGFβ], BRCA1, and Tax) (13, 14, 28, 34, 35, 41, 50, 53–56). However, the mechanism that controls *TERT* gene expression has not yet been completely elucidated, suggesting the existence of additional regulatory mechanisms. Furthermore, although we have shown using MMCT analysis that human chromosome 5 carries a *TERT* suppressor gene(s), the target gene(s) has not yet been identified from this chromosome (24, 39). Therefore, the identification of novel telomerase regulatory factors is eagerly anticipated to uncover the signaling mechanism that underlies the development of tumors.

Paired-like homeodomain 1 (PITX1) was described originally as a bicoid-related homeobox transcription factor that is recruited to regulate the transcription of the pro-opiomelanocortin (POMC) gene in the adult pituitary, and it is involved in the differentiation of pituitary cells and in pituitary formation (26). *PITX1* is expressed exclusively in the hind limb, not in the forelimb, and plays a crucial role throughout the process of limb development, and it also determines the morphology of muscle, tendon, and bones of the hind limb (11, 44). The development of oral epithelium, the first branchial arch, and its derivatives also are known to require *PITX1* (27, 45). *PITX1* was later identified as a suppressor of *RAS* activity and tumorigenicity based on an RNA interference (RNAi) library screen that induced the knockdown of the function of a wide range of genes. The knockdown of *PITX1* transcription resulted in a transforming activity and a phenotype that was comparable to that of *RAS* overexpression. It has since been shown that *PITX1* inhibits tumorigenicity by the downregulation of the *RAS* pathway through RAS protein activator-like 1 (*RASAL1*), which is a member of the family of RAS-GTP-activating factors (RAS-GAPs) that negatively regulate *RAS* activity. *RASAL1* has been shown to be a direct target of *PITX1* (23). However, the colony-forming ability of cells in which *RASAL1* is inhibited was significantly lower than that in which *PITX1* is inhibited, indicating that *RASAL1* is not the only target of *PITX1* that is responsible for the progression of tumorigenicity and for cell proliferation (23).

In this study, parental B16F10 cells, telomerase-negative B16F10 microcell hybrids with human chromosome 5 (B16F10MH5), and its revertant clones (MH5R) with reactivated telomerase were examined using cDNA microarray analysis to identify suppressor genes that carry telomerase repressor function. We report here on the identification of a possible candidate gene, *PITX1*, which is located on the human chromosome region 5q31 and which showed the inhibition of *TERT* transcription. *PITX1* directly binds to the *TERT* promoter via specific response elements, providing additional evidence that *PITX1* plays a significant role in the negative regulation of this promoter.

MATERIALS AND METHODS

Cell lines and cell culture. Mouse melanoma B16F10 cells and human melanoma A2058 cells were cultured in Dulbecco's modified Eagle's medium (DMEM; Sigma, St. Louis, MO) supplemented with 10% fetal bovine serum (FBS; HyClone, Logan, UT) at 37°C in a humidified incubator with 5% CO_2. The B16F10 microcell hybrids with an introduced human chromosome 5 were maintained in DMEM supplemented with 10% FBS and 800 μg/ml G418 (Calbiochem, La Jolla, CA).

Microarray analysis. Total RNA samples were isolated from the cells and were reverse transcribed and labeled using one-cycle target labeling and control reagents as instructed by Affymetrix. The quantitative analyses of gene expression were performed using Affymetrix human genome U133A and mouse genome 430A chips by following the manufacturer's instructions (Affymetrix, Santa Clara, CA). The chips were scanned using an Affymetrix scanner 3000. Expression values were calculated using Affymetrix Gene Chip analysis software MAS 5.0. All samples were analyzed in duplicate to confirm the reproducibility of the results.

STS content analysis. Three sequence-tagged site (STS) markers, located on human chromosome 5, were assigned for PCR analysis. The sequences of the forward and reverse primers are the following: *bac51529T*, 5′-TCTCGTTATG CTTTCCTCTCTAGAA-3′ and 5′-GACAGTTGTGTCCTGGTAGTCCA-3′; *D5S2474*, 5′-AAGGCCCAGTGGGAAAAG-3′ and 5′-TGAAATTTTCTTCTG TGACTCTACC-3′; and *D5S396*, 5′-CCCAGAATTAAACATGGTGA-3′ and 5′-TAGAGACAGTGTGCTGAGAGG-3′. The primers 5′-TCCACCAAGAGC TTCACCTT-3′ and 5′-CGGTGAGGTTGTTGATGTTG-3′ were used for *PITX1* detection. Thermocycling conditions were 30 cycles of denaturation for 1 min at 95°C, annealing for 30 s at 58°C, and extension for 1 min at 72°C. The amplified products were resolved on a 2% agarose gel.

RNA isolation, reverse transcriptase PCR, and qRT-PCR. Total cellular RNA was extracted using the RNeasy Minikit (Qiagen, Valencia, CA) and then was treated with RNase-free DNase I (Wako, Osaka, Japan) to remove residual genomic DNA. First-strand cDNA was synthesized from 2.3 μg of total RNA using an oligo$(dT)_{15}$ primer (Roche, Indianapolis, IN) and Moloney murine leukemia virus (MMLV) reverse transcriptase (Invitrogen, Carlsbad, CA) in accordance with the manufacturer's recommendations. *PITX1* mRNA expression was examined using the primers 5′-TCCACCAAGAGCTTCACCTT-3′ and 5′-CGGTGAGGTTGTTGATGTTG-3′. Thermocycling conditions were 30 cycles of denaturation for 30 s at 95°C, annealing for 45 s at 55°C, and extension for 30 s at 72°C for 30 cycles. The primers 5′-ATGTCACGGAGAGCACATTC-3′ and 5′-CTGCAGATGGGCATGGCTA-3′ were used for the detection of *mtert* mRNA expression, using 30 cycles of 30 s at 95°C, 45 s at 65°C, and 30 s at 72°C. The primers 5′-CGAGAGCAGACACCAGCAG-3′ and 5′-TTTTACTCCCAC AGCACCTC-3′ were used for the detection of *hTERT* mRNA expression, using 28 cycles of 30 s at 95°C and 60 s at 68°C. *GAPDH* was similarly amplified as an internal control. The products were visualized following electrophoresis on a 2% agarose gel. The real-time quantitative reverse transcription-PCR (qRT-PCR) was performed using an Applied Biosystems 7300 thermal cycler and a SYBR green PCR kit (Applied Biosystems, Foster City, CA).

The amplification was performed using 40 cycles. The SYBR green fluorescence signal was monitored in each cycle for the reference and marker genes.

Assay of telomerase activity. *PITX1* expressing- and parent vector-transfected B16F10 cells were harvested 48 h after transfection. Telomerase activity was assayed by the stretch PCR method using the TeloChaser telomerase assay kit (Toyobo, Osaka, Japan) according to the manufacturer's protocol.

Gene silencing by RNA interference. *PITX1* expression was inhibited using Dharmacon ON-TARGETplus smart pool PITX1 short interfering RNA (siRNA) (Latayette, CO). ON-TARGETplus nontargeting pool siRNA was used as a negative control. siRNAs were transfected by DharmaFECT 1 (Dharmacon), and cells were harvested 48 h after transfection and subjected to RT-PCR. The siRNA pool against *PITX1* includes CCAAACAGCACUCGUCGUU, GUGCAAGGGUGGCUACGUG, GGCGUAAGCGCGAGCGUAA, and CAACGUACGCACUUCACAA.

Plasmid construction. Various lengths of *hTERT* and *mtert* promoter regions (shown in Fig. 4A), which included the transcription start site, were PCR amplified from genomic DNA and were inserted into the Acc65I/BglII-digested luciferase (Luc) reporter vector pGL3-basic (Promega, Madison, WI). For the mutation of the constructs, a 6-nucleotide deletion in the *PITX1* binding site was introduced using a PCR-based site-directed mutagenesis kit (Toyobo). The *PITX1* expression and parent vectors were purchased from Origene (Rockville, MD). All of the plasmids were confirmed to have the correct sequence by DNA sequencing.

Luciferase assay. The cells were plated in 12-well plates 24 h before transfection. Reporter plasmids (0.25 μg) and effector plasmids (1.0 μg) were transfected using the Lipofectamine LTX reagent (Invitrogen) according to the manufacturer's protocol. pGL4.70-*renilla* (Promega) was cotransfected as an internal control. The cells were lysed 48 h after transfection and were subjected to a luciferase assay using the Picagene dual SeaPansy luminescence kit (Toyo Ink, Tokyo, Japan) according to standard protocols. All of the experiments were performed at least three times. Luciferase activity was calculated as the activity of the reporter constructs compared to the *Renilla* activity.

Western blot analysis. Lysates (20 μg of protein) were subjected to SDS-PAGE using a 12% resolving gel and then were transferred to a polyvinylidene difluoride (PVDF) membrane (Pierce, Rockford, IL). The membrane was blocked and incubated with the primary antibody against *PITX1* (Abcam, Cambridge, MA) and the secondary antibody according to the manufacturer's instructions. Immunoreactive bands were visualized using the ECL detection system (Pierce).

Electrophoretic mobility shift assay (EMSA). Nuclear extracts were prepared by the sequential lysis of the cells in hypotonic (10 mM HEPES, 10 mM KCl, 0.1 mM EDTA and EGTA, 1 mM dithiothreitol [DTT], and protease inhibitors) and hypertonic (20 mM HEPES, 0.4 M NaCl, 1.5 mM $MgCl_2$, 0.1 mM EDTA and EGTA, 1 mM DTT, and protease inhibitors) buffers. The probes used were the oligonucleotides 5′-CCTTTAAAAAGGCTTAGGGATCACTA-3′ (for PRE1) and 5′-ATCACTAAGGGGATTTCTAGAAGAGC-3′ (for PRE2).

The probes were labeled with [γ-^{32}P]ATP using the Megalabel kit (Takara Bio Inc., Shiga, Japan) and then were annealed with the corresponding antisense oligonucleotides. The binding reaction was performed using nuclear extracts (50 μg protein) in 20 μl binding buffer [8 mM HEPES, 2.5 mM Tris, 10% glycerol, 1 mM EDTA, 2.5 mM $MgCl_2$, 90 mM NaCl, 1 mM DTT, 0.5 μg of poly(dI-dC) · poly(dI-dC), and protease inhibitors]. The labeled probe (20,000 cpm) then was added, and the solution was incubated at room temperature for 30 min and then kept on ice. The products subsequently were subjected to electrophoresis on a 4% polyacrylamide gel. The gel was dried and exposed to X-ray film. For competition analysis, a mutant oligonucleotide, 5′-CCTTTAAAAAGGCGGAGGGATCACTA-3′ (for PRE1) or 5′-ATCACTAAGGGGCGTTCTAGAAGAGC-3′ (for PRE2), was added to the binding reaction mixture in a 500-fold excess compared to the amount of the probe and was incubated at room temperature prior to probe addition. For the supershift assay, the *PITX1* antibody or control IgG was added after the 30-min incubation with the probe, and the mixture then was incubated at room temperature for 10 min.

ChIP. The chromatin immunoprecipitation (ChIP) assay was performed according to a standard protocol. Briefly, to cross-link the DNA in chromatin to histones, the cells were incubated in 1% formaldehyde for 10 min at 37°C. After being washed with cold phosphate-buffered saline (PBS) containing protease inhibitors (Complete, EDTA free; Roche), the cells were resuspended in SDS lysis buffer (1% SDS, 10 mM EDTA, 50 mM Tris-HCl, with Complete). DNA then was broken into 200- to 1,000-bp fragments by sonication (Branson 250 microtip sonicator; Branson Ultrasonics, Danbury, CT). After dilution, resultant solutions containing the equivalent of 1×10^4 cells were used as an internal control (input). The remainder of the sample was immunoprecipitated using the *PITX1* antibody for 16 h at 4°C. Protein A-agarose (Upstate, Lake Placid, NY) then was used to collect the immunoprecipitated complexes, which were eluted using elution buffer (1% SDS, 0.1 M $NaHCO_3$, 10 mM DTT) after extensive washing. The cross-link then was reversed by the addition of 5 M NaCl, which was followed by protease K treatment. DNA was recovered using phenol-chloroform extraction and ethanol precipitation and was used as a template for PCR to amplify the region of the *PITX1* binding sites in the *TERT* promoter. The forward and reverse PCR primers used were 5′-TTTCCAAACCGCCCCTTT-3′ and 5′-CTGTCACGCTCGCTGGAG-3′ for *hTERT* and 5′-CAGTTCAGGCCCATATCTCC-3′ and 5′-TTTGGTGCCTTCAGCTTTCT-3′ for *mtert*. PCR conditions were 10 min at 95°C, followed by 33 cycles of 95°C for 20 s, 55°C for 20 s, and 72°C for 20 s, plus a final extension at 72°C for 1 min. The products were subjected to electrophoresis on a 2% agarose gel.

Immunohistochemistry. Immunohistological examination was performed on 16 surgically resected gastric adenocarcinomas. All specimens were extracted from the files of the Division of Organ Pathology, Faculty of Medicine, Tottori University, and affiliated teaching hospitals. Approval for the study was obtained from the Institutional Review Board of the Faculty of Medicine, Tottori University (approval number 283). All specimens were fixed with 10% formalin and embedded in paraffin. Three-micrometer-thick sections and a Histofine SAB-PO (R) immunohistochemical staining kit (Nichirei, Tokyo, Japan) were used for immunohistochemical analysis. Briefly, paraffin-embedded sections were dewaxed with xylene and gradually hydrated. Antigen retrieval was performed by autoclave in 10 mM citrate buffer (pH 6.0) for 10 min after endogenous peroxidase activity was blocked by immersing the slides in 0.3% hydrogen peroxide in methanol for 30 min. As primary antibodies, a rabbit polyclonal antibody raised against PITX1 (1:200; Abcam, Cambridge, MA) was used. Immunoreactions were visualized with diaminobenzidine, and the sections were counterstained with hematoxylin.

RESULTS

Expression microarray analysis of B16F10 microcell hybrids for identification of telomerase repressor genes on chromosome 5. To gain insight into telomerase suppressor genes on human chromosomes, we previously generated mouse melanoma B16F10 microcell hybrids containing individual normal human chromosomes using MMCT. We found that human chromosome 5 carries a putative telomerase repressor gene (24).

The strategy that we used to identify this putative telomerase repressor gene(s) on human chromosome 5 is outlined in Fig. 1. We compared the results of a cDNA microarray analysis of parental B16F10 cells, a B16F10 microcell hybrid that was telomerase negative and contained a human chromosome 5 (MH5), and its revertant clones (MH5R) that exhibited the reactivation of telomerase due to extended culture passages. We first sought to identify genes that are differentially expressed by human chromosome 5 in B16F10MH5 clones compared to MH5R clones using Affymetrix human genome U133A gene chips, which encompass about 22,000 transcripts of known genes. In this study, a signal $\log_2$ ratio (SLR) of 2 (fold change, ≥4) in duplicate experiments was used as an arbitrary cutoff for the determination of mRNA level changes. SLR indicates the absolute signal intensity that is calculated using the Affymetrix analysis software. The expression level of nine genes was increased more than 4-fold (SLR, ≥2) in the MH5 clone compared to that in control B16F10 cells or that in the MH5R clone. The MH5R clone showed expression levels similar to those of the control. Three of these nine genes localize to human chromosome 5. These genes, namely, the transforming growth factor beta-induced (*tgfβi*), elongation factor RNA polymerase II, 2 (*ell2*), and paired-like homeodomain 1 (*pitx1*) genes, also showed a lower expression in parental B16F10 cells than in MH5 clones when assessed using Affymetrix mouse genome 430A gene chips (Table 1).

To confirm the result of the microarray analysis, we inves-

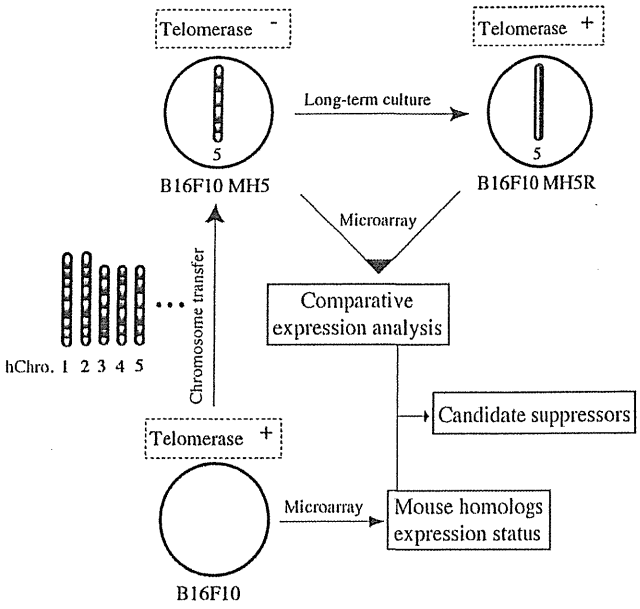

FIG. 1. Outline of the strategy used to identify negative regulators of telomerase. Normal human chromosomes were previously individually transferred into B16F10 cells. Only the introduction of human chromosome 5 (MH5) inhibited telomerase activity, which subsequently was reactivated during long-term culture (MH5R). Genes that were differentially expressed from human chromosome 5 between MH5 and MH5R were identified by cDNA microarray. Mouse homologs of these genes, which exhibited reduced expression in B16F10 cells, ultimately were chosen as candidate genes for further analysis.

tigated *PITX1*, *TGFβI*, and *ELL2* mRNA expression profiles in MH5 and MH5R clones using qRT-PCR. The mRNAs of *PITX1*, *TGFβI*, and *ELL2* were notably expressed in MH5 clones, in which *mtert* mRNA was barely detectable (Fig. 2A and B and data not shown). In contrast, the level of these mRNAs showed the reciprocal patterns in the parental cells and MH5R clones (Fig. 2A and B). Thus, the physiological expression of *PITX1*, *TGFβI*, and *ELL2* mRNA negatively correlated with *mtert* mRNA expression in the B16F10 clones.

TGFβI encodes a secreted protein, transforming growth factor β (TGFβ), that is known to be a regulator of telomerase activity through the repression of the *hTERT* gene (57). *ELL2* encodes a member of the ELL family of RNA polymerase II elongation factors. The elongation stage of transcription plays an important role in the regulation of gene expression. It has been reported that the ELL family, containing ELL2, also regulates cell proliferation and cell survival (22). *PITX1* has

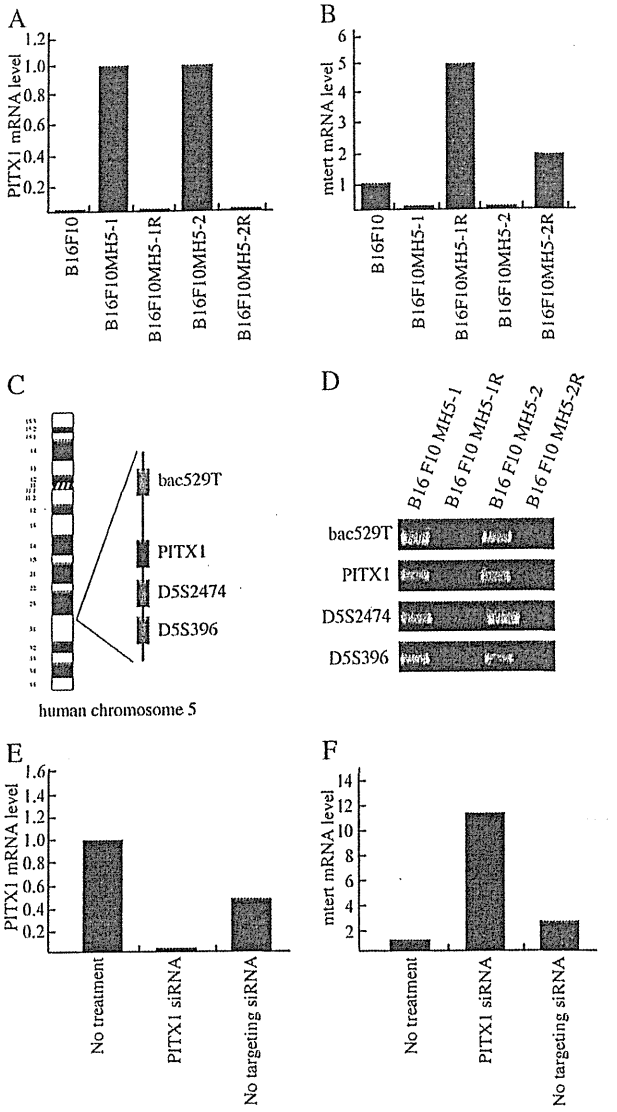

FIG. 2. Downregulation of *mtert* expression in MH5 clones is associated with *PITX1* expression. (A and B) Analysis of the mRNA expression of *PITX1* and *mtert* in microcell hybrids with human chromosome 5 (MH5) was performed using qRT-PCR. *GAPDH* was used as an internal control for each sample. MH5-1 and -2 showed strong repression of *mtert* expression, which was associated with the expression of *PITX1*. In contrast, revertant clones (MH5-1R and -2R) with telomerase activity showed reduced *PITX1* transcription. (C) Schematic diagram showing the location of the genomic loci of *PITX1* and flanking STS markers on human chromosome 5. (D) The chromosomal regions neighboring *PITX1* were not detected by genomic PCR in MH5R clones. (E and F) Depletion of *PITX1* by siRNA induces reactivation of *mtert* transcription in both MH5-1 and -2 clones in B16F10.

TABLE 1. Comparative expression of candidate telomerase suppressor genes analyzed using microarrays[a]

Gene name	Gene accession no.	Probe set name	Exp 1					Exp 2				
			B16F10 signal	MH5-1		MH5-1R		B16F10 signal	MH5-2		MH5-2R	
				Signal	SLR	Signal	SLR		Signal	SLR	Signal	SLR
TGFBI	NM_000358.1	201506_at	95.3 (A)	1,639.4 (A)	3.5 (I)	109.7 (A)	0.1 (NC)	92.4 (A)	1,287.4 (A)	2.6 (NC)	138.1 (A)	0.3 (NC)
PITX1	NM_002653.1	208502_s_at	145.7 (A)	1,616.5 (A)	2.7 (I)	243.6 (A)	0.1 (NC)	240.4 (A)	2,674.1 (A)	3.3 (I)	330.9 (A)	0.8 (NC)
ELL2	NM_012081.1	214446_at	198.2 (A)	2,818.8 (A)	3.6 (I)	784.2 (A)	1.5 (NC)	98.3 (A)	1,784.7 (A)	2.9 (I)	755.8 (A)	1.9 (I)

[a] The change in signal intensity for a specific probe between B16F10 and MH5 or MH5R is shown as either increased (I) or not changed (NC). SLR is a comparison between signal intensities for B16F10 parental cells and telomerase-negative or reactivated MH5 clones. The detection algorithm used probe set intensities to assign an absent (A), present, or marginal call.

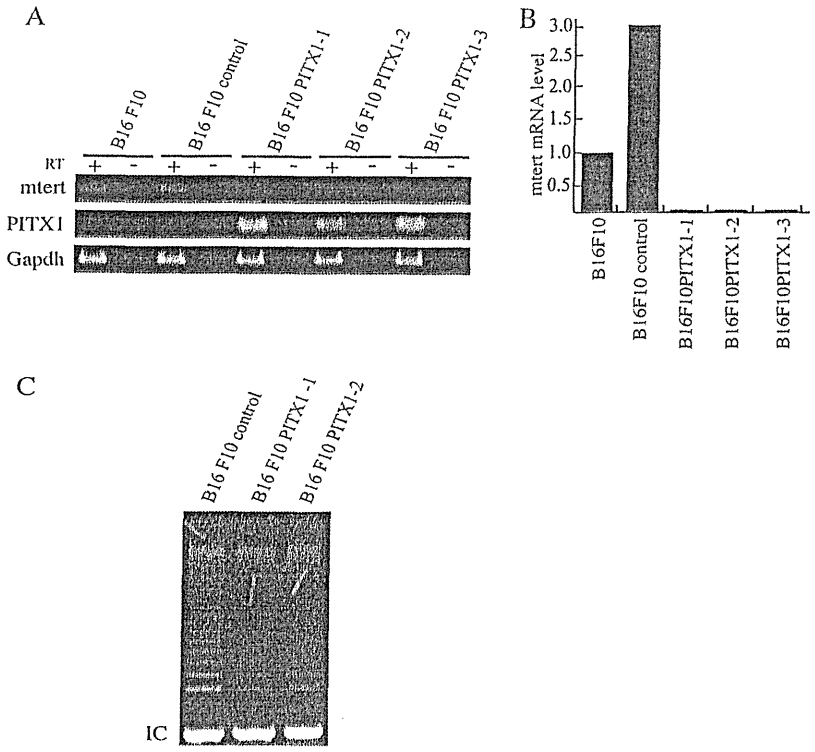

FIG. 3. Expression of *PITX1* inhibited *mtert* mRNA expression and telomerase activity in B16F10 cells. (A and B) RNA was prepared from B16F10 cells transfected with a *PITX1* expression vector or with control vector (*pcDNA3.1*) and was analyzed for *mtert* and *PITX1* mRNA expression using RT-PCR and qRT-PCR. (C) *PITX1* transfection resulted in depleted telomerase activity as assessed using the TeloChaser kit. IC is the internal control provided in the kit.

been reported to inhibit *RAS* activity and tumorigenicity, and it also induces the activation of the *p53* tumor suppressor gene in human breast cancer by directly binding to its promoter region (23, 29). These results suggest that the screening of the expression profiles of telomerase-positive and -negative MH clones of this study is an effective strategy for the identification of novel telomerase regulatory factors that are associated with cell proliferation.

Since little is known about the role of *PITX1* in the maintenance of telomerase enzyme activity, including the regulation of *TERT* transcription, we focused our study on *PITX1*.

Downregulation of *mtert* expression in MH5 clones is associated with *PITX1* expression profiles. We further compared the state of the genomic loci containing *PITX1* on the introduced human chromosome 5 in MH5 and MH5R clones by PCR analysis, using three chromosome 5-specific STS markers and a *PITX1*-specific primer (Fig. 2C). All of the loci examined (*bac51529T*, *D5S2474*, *D5S396*, and *PITX1*) were commonly deleted in MH5R, but not in MH5, clones (Fig. 2D). This result indicated that the observed decrease in *PITX1* mRNA expression is a result of either a deletion or a rearrangement of the genomic region harboring *PITX1* in the introduced human chromosome 5.

To further examine *mtert* suppression effects by *PITX1* under physiological conditions, we knocked down *PITX1* expression in MH5 clones that introduced human chromosome 5 in mouse melanoma B16F10 cells and human melanoma A2058 cells using RNAi. As shown in Fig. 2E and F, the depletion of *PITX1* leads to the reactivation of *TERT* RNA expression in both B16F10MH5 and A2058MH5 clones, suggesting that *PITX1* is a negative regulator of *TERT* transcription in both human and mouse (data not shown).

Expression of *PITX1* inhibits *mtert* transcription and telomerase enzymatic activity. To investigate the effect of *PITX1* expression on telomerase activity, we transfected B16F10 cells with an expression vector (pcDNA3.1-*PITX1*) containing the full-length *PITX1* coding sequence or with a negative-control empty vector and assayed the subsequent mRNA expression of *mtert* using RT-PCR and qRT-PCR. As shown in Fig. 3A and B, the expression of *PITX1* resulted in a dramatic reduction in *mtert* mRNA expression. In contrast, *mtert* mRNA expression was similar to that of parental B16F10 cells in cells transfected with the empty vector. These findings suggested that *PITX1* can somehow suppress *mtert* mRNA expression in B16F10 cells.

The level of *TERT* transcription most commonly is regulated in a telomerase enzyme activity-dependent manner. Therefore, we next measured the effect of *PITX1* transfection on telomerase activity using a telomerase activity detection kit (TeloChaser) that is based on the stretch PCR method. B16F10 cells transfected with *PITX1* showed significantly reduced telomerase activities compared to that of the corresponding parental cells (Fig. 3C). These results suggest that the mechanism by which *PITX1* suppresses *mtert* mRNA expression involves the inhibition of telomerase activity.

PITX1 inhibits telomerase enzymatic activity through the regulation of *TERT* promoter activity. To investigate whether *PITX1* inhibits *TERT* mRNA expression through the modula-

tion of TERT promoter activity, we constructed a mouse *tert* promoter-luciferase reporter plasmid (pGL3) containing a 1,955-bp fragment (mtert1955) from within the *mtert* promoter region or various truncated fragments (mtert1747, mtert824, mtert356, and mtert155) of the 5′ region of the *tert* gene (Fig. 4A). We then examined the effect of transient *PITX1* cotransfection with these pGL3-mtert-Luc reporters, or with an empty pcDNA3 control vector, into mouse B16F10 cells on the transcriptional activity of these *tert* promoters by the measurement of Luc reporter activity (Fig. 4A). The expression of *PITX1*, but not parental vector transfection, decreased the promoter activity of mtert1955 and mtert1747 by 60% ($P < 0.01$) and that of mtert824, mtert356, and mtert155 by 40% (Fig. 4A). These data suggest that *PITX1* directly regulates *mtert* transcription, and that the *mtert* promoter region between −1747 and −824 is critical for *PITX1* suppression.

Genomatrix and sequence analysis has identified potential *PITX1* binding sites within the *PITX1* transcription factor regulatory element (PRE) as the sequences TAA(T/G)CC [GG(C/A)TTA in reverse], AAATCC (GGATTT in reverse), and TAATCC (GGATTA in reverse) (23). In this report, these sites are designated PRE1, PRE2, and PRE3, respectively (Fig. 4B). We identified two PRE2 sites (−1850/−1845 and −273/−268) and one PRE3 site (−1100/−1095) in the *mtert* promoter region and one each of the PRE1 (−1366/−1361), PRE2 (−1344/−1339), and PRE3 (−1322/−1317) sites in the *hTERT* promoter region (Fig. 4B).

The Luc reporter experiments using fragments of the *mtert* promoter suggested that the PRE3 present in the −1100 region of the *mtert* promoter is responsible for the suppressive effect of *PITX1*. To further examine this possibility, we first generated *mtert* mutant promoter plasmids (mtert1955mut3) in which the sequence of PRE3 in mtert1955 was deleted (Fig. 4C). This mutation of PRE3 reduced *mtert* promoter activity to 20% of that of parental mtert1955 and gave the same level of promoter activity as that of the truncated fragments mtert824, mtert356, and mtert155 (Fig. 4A and D). We next constructed mutant mtert promoter reporter plasmids in which either one PRE2 site (mtert1995mut2L), two PRE2 sites (mtert1955mut2), or one PRE3 site (mtert1995mut3) was deleted. The reporter plasmid containing the PRE3 mutation showed a significant recovery of *mtert* transcriptional activity compared to that of the PRE2 mutation (mtert1955mut2L and mut2) and wild-type reporter ($P < 0.01$) (Fig. 4C and D). In addition, the result of suppression effect by PRE mutation was similar to that of the short type of *mtert* reporter plasmids (mtert1747) (data not shown). Although we cannot rule out the possibility that another mechanism(s) of *mtert* transcription also is involved, PRE3 in the *mtert* promoter may play a crucial role in the regulation of *mtert* transcription. Thus, this result suggested that *PITX1* can inhibit *mtert* transcription through the *mtert* promoter.

We next determined whether the *hTERT* promoter is regulated by *PITX1* in a manner similar to that of the *mtert* promoter. Sequence analysis indicated that only a region of approximately 300 bp is highly conserved between the *hTERT* and the *mtert* promoters (Fig. 4E). Interestingly, all three PRE sites of the *hTERT* promoter lie within this conserved region, suggesting that this region also plays a significant role in the regulation of *hTERT* transcription. To test this prediction, two luciferase reporter plasmids were prepared in which the promoter activity of 1.4 (hTERT1412)- and 1.0 (hTERT1047)-kbp fragments of the *hTERT* promoter, with and without PRE sites, respectively (Fig. 4A), was examined following the cotransfection of *PITX1* in B16F10 cells. Luciferase assays indicated that cotransfected *PITX1* decreased the promoter activity of hTERT1412 by 60% ($P = 0.0001$) and that of hTERT1047 by 40% compared to that of the parent vector (Fig. 4A). This result indicated that *PITX1* also affects *hTERT* transcriptional activity through PRE sites.

To confirm that the decreased *hTERT* promoter activity induced by *PITX1* in mouse cells also could occur in human cells, the luciferase reporter assays using transiently cotransfected hTERT1412 or hTERT1047 and *PITX1* were repeated using a human melanoma cell line, A2058, which also lacks endogenous *PITX1* expression (data not shown). As shown in Fig. 5A, *PITX1* also induced a decrease in hTERT1412 promoter activity in these cells that was 1.9-fold less ($P = 0.01$) than the activity of the hTERT1047 promoter, indicating that *PITX1* also regulates *hTERT* promoter activity in humans. To further analyze the *PITX1* modulation of the *hTERT* promoter in A2058 cells, we constructed, and similarly analyzed, mutant *hTERT* promoter reporter plasmids in which either PRE1 (*hTERT1412mut1*), PRE2 (*hTERT1412mut2*), or PRE3 (*hTERT1412mut3*) was disrupted by changing the sequence from 5′-GGCTTA-3′ to 5′-AGCTTA-3′, from 5′-GGATTT-3′ to 5′-AAATTT-3′, or from 5′-GGATTT-3′ to 5′-AGATGT-3′, respectively (Fig. 5B). The mutation of any of these PREs resulted in a 2- to 2.1-fold increase in *hTERT* promoter activity compared to that of the parental *hTERT1412* (Fig. 5C), indicating that these PREs are essential for the *PITX1* modulation of *hTERT* promoter activity. These findings suggest that the suppression of *hTERT* promoter activity by *PITX1* is dependent exclusively on *PITX1* consensus binding sites in the promoter. Therefore, these PRE sites may play a crucial role in the regulation of *hTERT* promoter activity.

PITX1 directly binds to the *TERT* promoter *in vitro* and *in vivo*. To determine whether *PITX1* directly binds to the *hTERT* promoter, we performed EMSA using nuclear extracts prepared from parental B16F10 and *PITX1*-transfected B16F10 cells. Western blotting confirmed that the PITX1 protein was expressed in *PITX1*-transfected B16F10 cells (Fig. 6A). We then assayed the binding of PITX1 to DNA probes containing either PRE1 or PRE2 of the *hTERT* promoter using an EMSA (Fig. 6B and C, respectively). Each probe formed a complex with PITX1. Although some background signals were detected in the parental B16F10 lysate (Fig. 6B and C, lane 2), PITX1 did form complexes with the labeled probes PRE1 and PRE2, which were abrogated by excess unlabeled wild-type probe but not by mutated probes (Fig. 6B and C, lanes 5 to 7). To verify the specificity of the *PITX1*-DNA interaction, we performed a supershift EMSA using the PITX1 antibody. As shown in Fig. 6D, the complexes (P) formed by PITX1 with the PRE1 (left) or PRE2 (right) probe were attenuated by a specific anti-PITX1 antibody but not by control IgG. These results indicate that PITX1 directly binds to both PRE1 and PRE2 within the *hTERT* promoter *in vitro*.

To determine whether PITX1 could bind to the PRE regions of the *hTERT* or *mtert* promoter within cells, we carried out ChIP assays using the human and mouse melanoma cell lines, A2058 and B16F10, respectively, that were transiently trans-

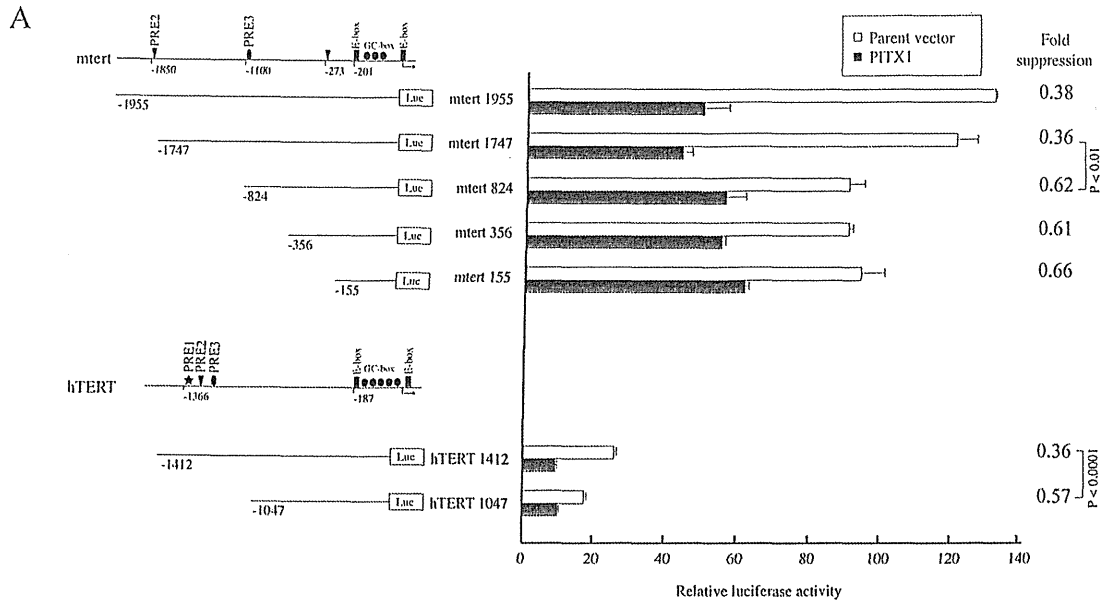

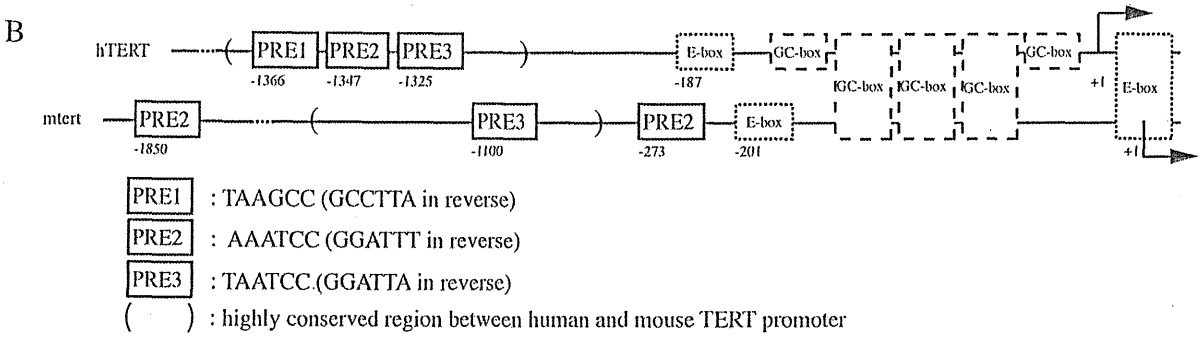

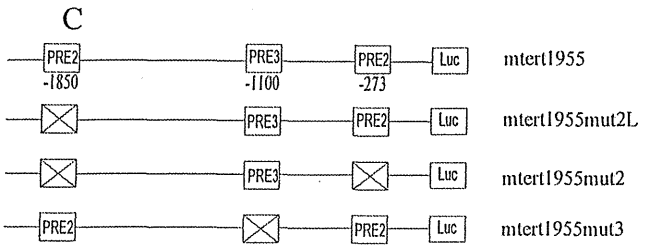

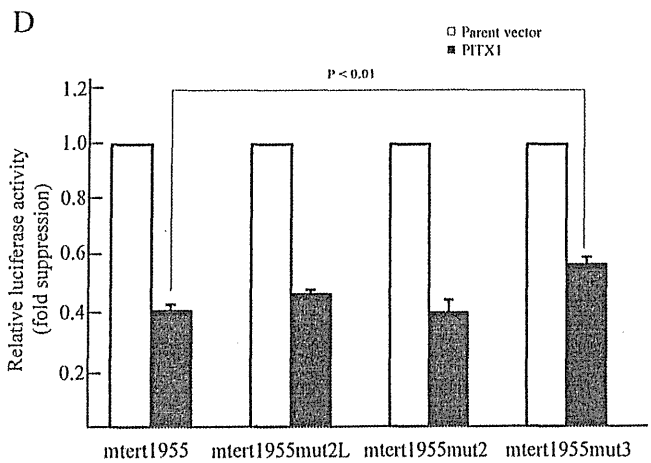

E

```
hTERT  -1495 TGTTTTCTATGTTGGCTTCTCTGCAGAGAACCAGTGTAAGCTACAACTTAACTTTTGTTGGAACAAATTTTCCAAACC--GCCCCTTTGCCCTA-GTGGC -1399
             ********** *** **** **  * **** *   **** *  * *** *   ******* * ******  **    *  **** * *  **** ** **
mtert  -1267 TGTTTTCTATGCTGGTTTCTTTG--GGGAACTACACTAAGGT--AGCTTCA---TTGTTGGCATAAATTTCTCAGTTCAGGCCCATATCTCCTAAGTAGC -1175

                                                PRE1                PRE2                PRE3
       -1398 AGAGA----CAATTCACAAACACAGCCCTTTAAAAAGGCTTAGGGATCACTAAGGGGATTTCTAGAAGAGCGACCCGTAATCCTAAGTATTTACAAGACG -1303
             ***      *** ** ****** * *** * ****** ** * *   ******  *** ***** ** ***  ** ******** ** ********* *
       -1174 AGAACTAAGCAAATCTCAAACA-AACCCCTCAAAAAGACTGATG-TCCACTAAACGGACTTCTAAAATAGC-TCCTGTAATCCTGAGCATTTACAAGGC- -1079
                                                                                    PRE3
       -1304 AGGCTAACCTCCAGCGAGCGTGACAGCCCAGGGAGGGTGCGAGGCCTGTTCAAATGCTAGCTCCATAAATA-AAGCAATTTCCTCCGGCAGTTTCTGAAA -1204
              ***  ******    ** * *  *       **    ***   ********** ** *  *** ********** * **   *****
       -1078 -GGCAGACCTCCTATAAGGGAGTAAATAT---GAAAACGCG---CCTGTTCAAATGCTAGGTCGGTGGATAGAAGCAATTTCCTCAGAAAG---CTGAAG  -989

       -1205 GTAGGAAAGGTTACATTTAAGGTTGCGTTTGTTAGCATTTCAGTGTTTGCCGACCTCAGCTACAG -1138 hTERT
             *          **   ******   ********************** * **********
        -988 G-----------CACCAAAGGTTATATTTGTTAGCATTTCAGTGTTTGCCAAACTCAGCTACAG  -935 mtert
```

fected with *PITX1* in B16F10 and A2058 cells and MH5 clones. The promoter region that contains PRE1, PRE2, and PRE3 sites in *hTERT* and the PRE3 site in *mtert* was specifically amplified by PCR from chromatin that was precipitated with the anti-PITX1 antibody from all cell types (Fig. 7 and data not shown). These findings suggest that PITX1 can directly bind to the *TERT* promoter *in vivo*.

Expression of *PITX1* protein in human resected gastric normal mucosa and carcinoma tissue specimens. It has been reported that *PITX1* expression is reduced in various types of human cancers, including gastric, bladder, and colon cancers (4, 5). To provide further direct evidence that *PITX1* expression levels are related to human cancer, we examined *PITX1* expression in 16 surgically resected gastric adenocarcinoma specimens by immunohistochemistry. We found that *PITX1* was expressed on the sections of nontumoral gastric mucosae of all 16 specimens. In contrast, 70% of samples (11/16) showed *PITX1*-negative staining on the carcinoma sections (Fig. 8). Thus, these findings strongly support the hypothesis that the downregulation of *TERT* by *PITX1* plays a crucial role in the multistep process of neoplastic development.

DISCUSSION

Using MMCT into the mouse melanoma cell line B16F10, we previously provided evidence to suggest that many tumor suppressor genes are involved in the multistep process of neoplastic development (24). B16F10 microcell hybrids with an introduced normal human chromosome 5 displayed the inhibition of telomerase activity due to a reduction in the level of *mtert* mRNA. We have reported recently that the introduction of human chromosome 5 showed a remarkable decrease in the growth rate and eventually cellular senescence in human A2058 melanoma cells. Moreover, this phenomenon also was accompanied by a reduction of *hTERT* expression and telomerase activity (39). In this study, using comparative microarray analyses and assays of promoter function and binding, we identified *PITX1* as a telomerase repressor gene on human chromosome 5 that directly regulates *hTERT* transcription. *PITX1* is located at the chromosome region 5q31 (9). The loss of a specific region of chromosome 5q31 has been observed in several types of human cancers, such as acute monocytic leukemia (AML) and esophageal and breast cancer cells (3, 21, 40). We explored the *PITX1* tumor expression profile using the ONCOMINE cancer microarray database (42). The results showed that *PITX1* expression is reduced in Barrett's esophagus and is significantly reduced during progression to Barrett's-associated adenocarcinoma (30). This phenomenon also is observed in lung, gastric, and colon cancer cells as well as tumor tissues of prostate and bladder but not in the respective normal tissues (4, 5, 23, 40, 46). In addition, the disappearance of *PITX1* was observed in 70% of gastric adenocarcinoma specimens (Fig. 8). Moreover, the suppression of *PITX1* expression by siRNA results in the reactivation of endogenous *TERT* expression in MH5 clones (Fig. 2E and F). Thus, these findings provide evidence that dysfunctions of the *PITX1* gene play an important role in the development of various types of human cancers.

Although a putative telomerase repressor gene was mapped to human chromosome bands 5p11 to 5p13 by a combination of functional analysis using the transfer of subchromosomal transferable fragments of chromosome 5 into B16F10 cells and by the deletion mapping of revertant clones with reactivated telomerase activity, the *PITX1* gene that we found to be a negative regulatory factor for *hTERT* in this study was located in the chromosome 5q31 region (38). It is possible that this large discrepancy between the mapping information for a candidate gene and the actual *PITX1* chromosomal localization is due to the scale of the screen used to identify the responsible gene. We used only 21 chromosome 5-specific STS markers to identify the location of the telomerase repressor gene. However, we do not rule out the possibility that there is another telomerase repressor gene that is located in the 5p11 to 5p13 region.

The overexpression of *PITX1* resulted in *p53*-dependent cell cycle arrest and apoptosis in the human mammary carcinoma cell line MCF-7 (29). *PITX1* has been shown to activate *p53* transcription via direct binding to the *p53* promoter. Moreover, *p21* and the placental transforming growth factor β gene (*PTGF*β), known as *p53* downstream target genes, were modulated by *PITX1* in a gene dosage-dependent manner, and *PTGF*β is known to inhibit tumor cell growth in the *TGF*β signaling pathway (29, 50). In addition, since *p53* can physically interact *in vivo* with *Smad2*, which is required for *TGF*β responses (8), it is likely that the modulation of the transcriptional activation of *p53* by *PITX1* enhances the activity of the *TGF*β signaling pathway by a number of mechanisms. However, *PITX1* still can induce apoptosis even in *p53*-depleted

FIG. 4. Luciferase assay of various truncated *hTERT* and *mtert* promoters in *PITX1*- and control vector-transfected B16F10 cells. (A) The schematic drawing (left) shows the position of the truncation site of each of the reporter plasmids. The firefly luciferase activity was standardized using *Renilla reniformis* luciferase activity from cotransfected pGL4.70. The promoter region that contains PREs significantly inhibits, and is therefore crucial for, *TERT* transcriptional activity in both humans and mice. Error bars represent standard deviations from three experiments. Statistical analysis (*t* test) using SigmaPlot 2000 and indicating a significant difference is shown (*P* values). (B) Comparison of transcription factor binding sequences in the *hTERT* and *mtert* promoters. The proximal promoter region of *hTERT* is partially similar to that of *mtert*, containing both E and GC boxes. The transcription start site is indicated by an arrow. Candidate *PITX1* binding sequences are indicated as *PITX1* response elements (PRE1, PRE2, and PRE3). (C) Schematic diagram showing the luciferase reporter plasmids that encode wild-type and PRE3-mutated versions of a fragment of the *mtert* promoter region. The crossed box represents mutation. (D) *PITX1* expression vectors were cotransfected with the mtert reporter plasmids shown in panel C and mtert 824, which lacks PRE3, and promoter activity was assayed using a luciferase assay. The firefly luciferase activity was standardized using *Renilla reniformis* luciferase activity from cotransfected pGL4.70. The transfection of control vector was used as a suppression control to normalize the effect of *PITX1* transfection. The transcriptional activity of *mtert* was suppressed by the wild-type reporter compared to that of the mutated reporters. Error bars represent the standard deviations from three experiments. Statistical analysis (*t* test) using SigmaPlot 2000 and indicating a significant difference is shown (*P* values). (E) The sequences within the *TERT* promoter conserved between human and mouse. Three and one PRE sites of the *hTERT* and *mTERT* promoters lie within this conserved region.

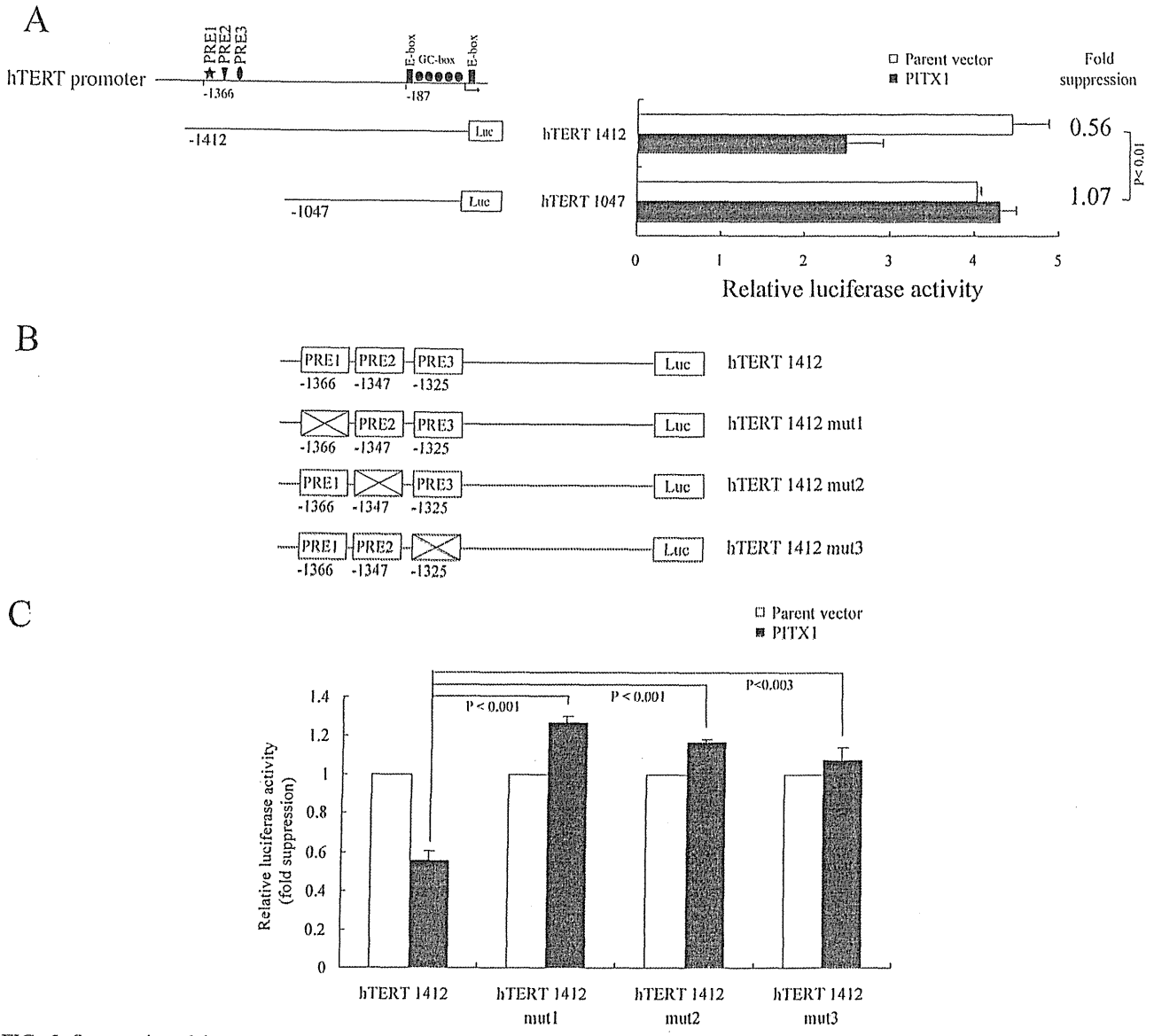

FIG. 5. Suppression of the transcriptional activity of the *hTERT* promoter by *PITX1*. (A) *PITX1* expression vectors were cotransfected into the human melanoma cell line A2058 with reporter plasmids containing a wild-type (*hTERT1412*) or a truncated (*hTERT1047*) *hTERT* promoter region in which the PRE site in the *hTERT* promoter region is eliminated. The resulting firefly luciferase activity was standardized using the *Renilla reniformis* luciferase activity from cotransfected pGL4.70. The transcriptional activity in *hTERT1412* indicated suppression effects that were approximately 2-fold greater than those of *hTERT*1047. Error bars represent the standard deviations from three experiments. Statistical analysis (*t* test) using SigmaPlot 2000 and indicating a significant difference is shown (*P* values). (B) Schematic diagram showing the luciferase reporter plasmids that carry wild and mutated versions of the *mtert* promoter region. The crossed box represents mutation. (C) *PITX1* expression vectors were cotransfected with reporter plasmids containing the wild-type or PRE-mutated versions of the *hTERT* promoter. The transcriptional activity of *hTERT* was suppressed by the wild-type reporter compared to that of the mutated versions. Error bars represent the standard deviations from three experiments. Statistical analysis (*t* test) using SigmaPlot 2000 and indicating a significant difference is shown (*P* values).

MCF-7 cells (29), suggesting the possibility that *hTERT* inhibition by *PITX1* is not the only mechanism by which *p53* causes telomerase inhibition.

Using MMCT, we and other investigators found that telomerase repressor genes are located on least four different human chromosomes, 3, 5, 6, and 10 (10, 20, 24, 32, 36, 47), suggesting that there are multiple telomerase-dependent pathways for the regulation of cellular senescence (37). It is likely that defects in these pathways are required for complete cellular immortalization and to predispose cells to neoplastic transformation.

There are some significant differences in telomere regulation between human and mouse biology. In particular, mouse telomeres are, on average, much longer than those in humans. Moreover, the expression of *hTERT* is more tightly regulated than that of *mtert* in normal somatic cells, although the expression of both genes is strongly upregulated in tumors. A transgenic mouse carrying a *lacZ* gene driven by the *hTERT* promoter has shown that the activity of the *hTERT* promoter in normal mouse tissues recapitulates the expression of the *hTERT* gene in normal human tissues (43). Furthermore, the

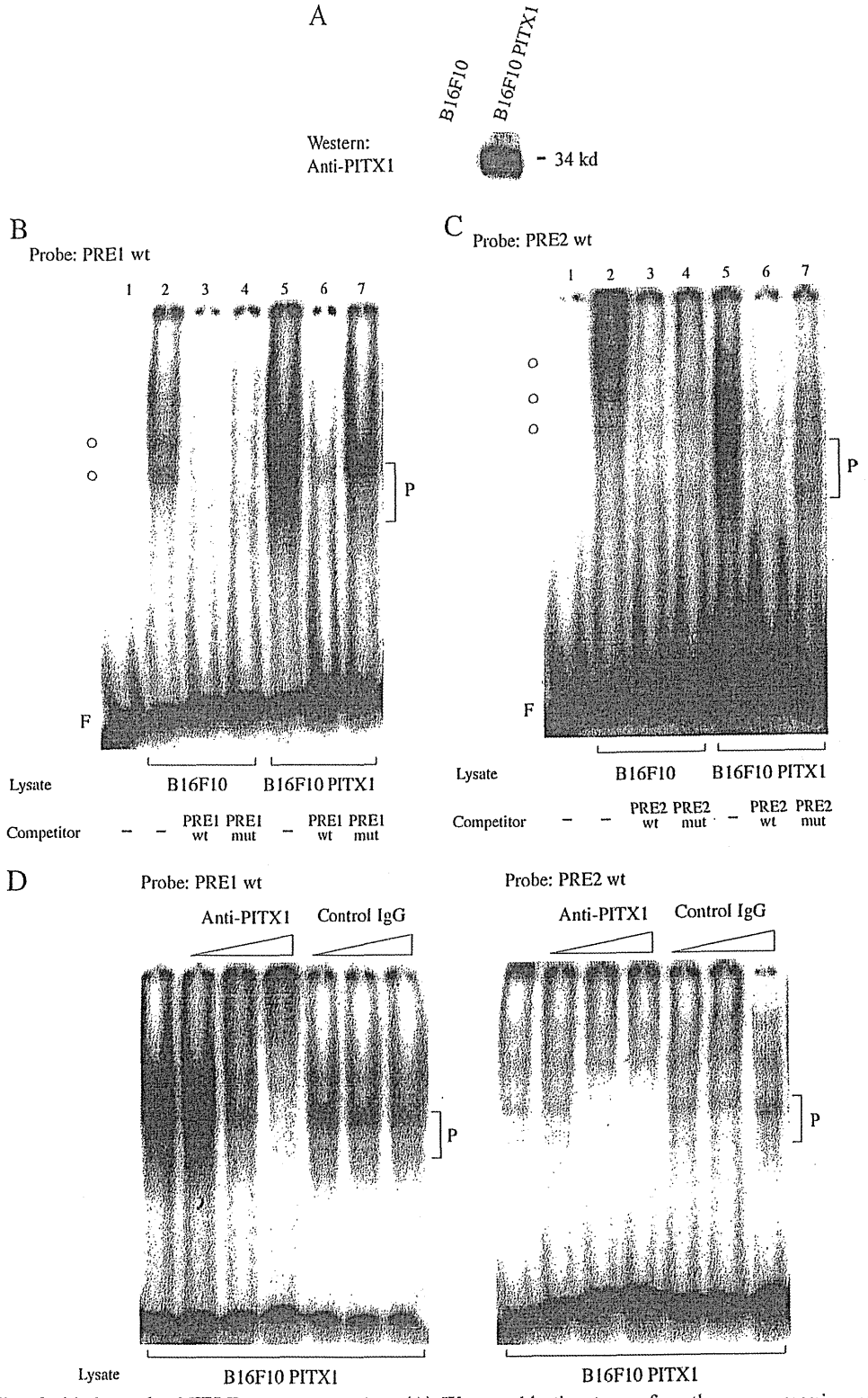

FIG. 6. *PITX1* directly binds to the *hTERT* promoter *in vitro*. (A) Western blotting to confirm the overexpression of PITX1 protein in B16F10-transfected cells. (B and C) EMSA was performed using the human PITX1 protein and a radiolabeled oligonucleotide probe designed to detect the binding of PITX1 to PRE1 (B) or PRE2 (C). The open circles indicate background signals. P indicates probe binding to PITX1. F, free probe; wt, wild type; mut, mutation; −, no competitor. (D) A supershift assay using the PITX1 antibody or control IgG. Triangles indicate increasing amounts of antibody.

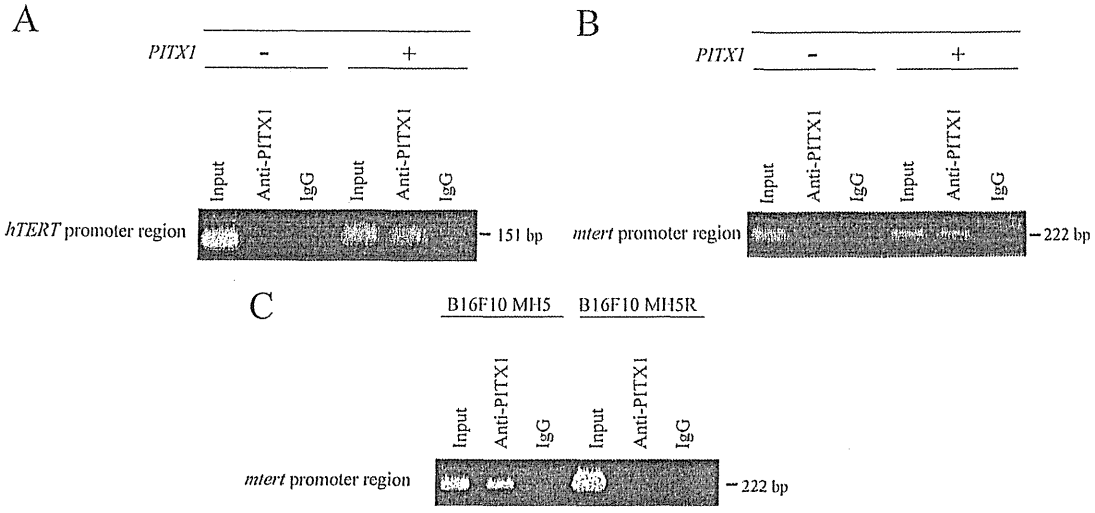

FIG. 7. *PITX1* directly binds to both the *hTERT* and the *mtert* promoter *in vivo*. A ChIP assay was carried out using the anti-PITX1 antibody to verify the binding of PITX1 to the *hTERT* and *mtert* promoters in human A2058, mouse B16F10 cells, and the B16F10MH5 clone. *PITX1* expressed in human- and mouse-transfected cells and B16F10MH5 clone was cross-linked to DNA using an anti-*PITX1* antibody. Rabbit immunoglobulin (IgG) was used as a negative control. Input represents PCR of the *hTERT* promoter DNA before immunoprecipitation.

expression of the *hTERT* transgene from a bacterial artificial chromosome containing the entire *hTERT* gene that was introduced into a mouse also was more similar to that of endogenous *hTERT* in humans than to that of endogenous *mtert* (19). Consistently with these findings, our results provide further evidence that the activity of the *hTERT* promoter is under tighter control than that of *mtert*, even in mouse cancer cells (Fig. 4A). These results suggest that specific transcriptional inhibitors in human cells are very important for the strict control of the *hTERT* promoter.

It is known that several elements that are binding sites for transcriptional activators and inhibitors are conserved between the *hTERT* and the *mtert* promoters. In particular, two E boxes and three GC boxes are extremely similar between *hTERT* and *mtert* (Fig. 4B). These boxes lie within the proximal core promoter that is responsible for essential transcriptional activity (33, 49). In contrast, the 5′-flanking sequence of the core promoter is remarkably different between human and mouse (49). Interestingly, the overexpression of the transcription factor activator protein 1 (AP-1) was reported to suppress *hTERT* transcription by directly binding to two sites on the distal promoter of *hTERT* that are missing from the *mtert* promoter. Although the *mtert* promoter includes other putative AP-1 binding sites, AP-1 overexpression has no effect on *mtert* expression (49). Additionally, two nonconserved GC-boxes exist in the *hTERT* core promoter (Fig. 4C), only one of which was identified as a human-specific repressive element of the *Sp1/Sp3* complex (19). This box is located next to the transcription start site. In the present study, we found a promoter region that was highly conserved between *hTERT* and *mtert* promoters. Of the three candidate *PITX1* binding sites (PRE1, PRE2, and PRE3), only PRE3 exists within this conserved *hTERT* and *mtert* promoter region (Fig. 4B and E). The functional analysis of the *TERT* promoter activity of promoter constructs with mutations in the PRE sites and with various truncations of the promoter region indicated that these promoter disruptions abolished the ability of *PITX1* to repress transcription from the promoter in both human and mouse cells (Fig. 4 and 5). In addition, the inhibition of the complex formed between *PITX1* and PRE1 or PRE2 was observed using an excess of PRE1 and

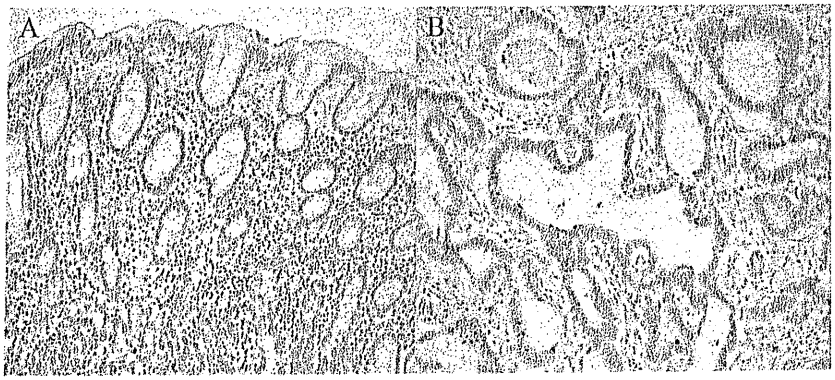

FIG. 8. Detection of *PITX1* protein by immunohistochemistry in gastric mucosa and adenocarcinoma. (A) *PITX1*-positive cells exist in surface mucous cells and fundic glands. (B) In contrast, *PITX1*-positive cells were not observed in carcinoma lesions.

PRE2 probes but not with a PRE3 probe (data not shown) in EMSA, indicating that *PITX1* binds with higher affinity to PRE1 and PRE2 than to PRE3. Thus, these data indicated that the conserved *TERT* promoter region containing PRE sites plays a crucial role in the regulation of *TERT* transcription by *PITX1*, and that the binding affinity of *PITX1* is of different strength for different PRE sites. Further investigation involving a detailed analysis of the *PITX1* affinity of binding to the *TERT* promoter and/or identification of *PITX1* targeting factors may be a great help in understanding the molecular mechanism by which telomerases are differentially regulated in humans and mice.

In accordance with its continued expression in tumor cells, telomerase expression also is maintained in most stem cells, as it is required for the self-renewal ability of stem cells. However, *hTERT* expression is strongly suppressed during differentiation, which contrasts sharply with the moderate downregulation of *mtert*. A recent study has provided evidence that the chromatin environment is a crucial factor for the tight regulation of *hTERT* transcriptional activity in human somatic cells (52). Endogenous *hTERT* and its downstream gene locus, but not the *mtert* gene, are located in a condensed chromatin domain in differentiated cells (52). That study also indicated that condensed chromatin could cooperate with transcriptional repressors on the promoter to effectively reduce the expression of *hTERT* during cell differentiation. It will be of interest to examine if *hTERT* suppression by *PITX1* is involved in stem cell differentiation and to determine the relationship between *PITX1* regulation and chromatin status.

In summary, we have provided evidence that MMCT studies incorporating chromosome mapping by positional cloning strategies, combined with expression profiling analysis, are an effective approach for the identification of tumor suppressor genes, such as negative regulators of telomerase. Our study demonstrated that *PITX1* is a negative regulator of telomerase through the transcriptional repression of the *TERT* promoter. However, the mechanism by which the function of *PITX1* contributes to the transcriptional silencing of the *TERT* gene remains to be clarified. Therefore, future studies that include the functional analysis of proteins or genes that associate with *PITX1* should facilitate our understanding of the molecular mechanisms that are involved in telomerase-dependent senescence or in cancer development.

ACKNOWLEDGMENTS

This study was supported by a Grant-in-Aid for Scientific Research (C) (22501012), (B) (20310120), and the 21st Century COE program from the Ministry of Education, Culture, Sports, Science, and Technology of Japan.

REFERENCES

1. **Artandi, S., et al.** 2002. Constitutive telomerase expression promotes mammary carcinomas in aging mice. Proc. Natl. Acad. Sci. U. S. A. 99:8191–8196.
2. **Blasco, M.** 2005. Telomeres and human disease: ageing, cancer and beyond. Nat. Rev. Genet. 6:611–622.
3. **Cavalli, L. R., R. B. Riggins, A. Wang, R. Clarke, and B. R. Haddad.** 2010. Frequent loss of heterozygosity at the interferon regulatory factor-1 gene locus in breast cancer. Breast Cancer Res. Treat. 121:227–231.
4. **Chen, Y., et al.** 2007. Decreased PITX1 homeobox gene expression in human lung cancer. Lung Cancer 55:287–294.
5. **Chen, Y. N., H. Chen, Y. Xu, X. Zhang, and Y. Luo.** 2008. Expression of pituitary homeobox 1 gene in human gastric carcinogenesis and its clinicopathological significance. World J. Gastroenterol. 14:292–297.
6. **Chiu, C., and C. Harley.** 1997. Replicative senescence and cell immortality: the role of telomeres and telomerase. Proc. Soc. Exp. Biol. Med. 214:99–106.
7. **Collins, K., and J. Mitchell.** 2002. Telomerase in the human organism. Oncogene 21:564–579.
8. **Cordenonsi, M., et al.** 2003. Links between tumor suppressors: p53 is required for TGF-beta gene responses by cooperating with Smads. Cell 113: 301–314.
9. **Crawford, M. J., et al.** 1997. Human and murine PTX1/Ptx1 gene maps to the region for Treacher Collins syndrome. Mamm. Genome 8:841–845.
10. **Cuthbert, A. P., et al.** 1999. Telomerase repressor sequences on chromosome 3 and induction of permanent growth arrest in human breast cancer cells. J. Natl. Cancer Inst. 91:37–45.
11. **DeLaurier, A., R. Schweitzer, and M. Logan.** 2006. Pitx1 determines the morphology of muscle, tendon, and bones of the hindlimb. Dev. Biol. 299: 22–34.
12. **Doherty, A. M., and E. M. Fisher.** 2003. Microcell-mediated chromosome transfer (MMCT): small cells with huge potential. Mamm. Genome 14:583–592.
13. **Fujimoto, K., et al.** 2000. Identification and characterization of negative regulatory elements of the human telomerase catalytic subunit (hTERT) gene promoter: possible role of MZF-2 in transcriptional repression of hTERT. Nucleic Acids Res. 28:2557–2562.
14. **Gabet, A., et al.** 2003. Inactivation of hTERT transcription by Tax. Oncogene 22:3734–3741.
15. **González-Suárez, E., J. Flores, and M. Blasco.** 2002. Cooperation between p53 mutation and high telomerase transgenic expression in spontaneous cancer development. Mol. Cell. Biol. 22:7291–7301.
16. **González-Suárez, E., et al.** 2001. Increased epidermal tumors and increased skin wound healing in transgenic mice overexpressing the catalytic subunit of telomerase, mTERT, in basal keratinocytes. EMBO J. 20:2619–2630.
17. **Hahn, W. C., et al.** 1999. Creation of human tumour cells with defined genetic elements. Nature 400:464–468.
18. **Harley, C., A. Futcher, and C. Greider.** 1990. Telomeres shorten during ageing of human fibroblasts. Nature 345:458–460.
19. **Horikawa, I., et al.** 2005. Differential cis-regulation of human versus mouse TERT gene expression in vivo: identification of a human-specific repressive element. Proc. Natl. Acad. Sci. U. S. A. 102:18437–18442.
20. **Horikawa, I., M. Oshimura, and J. Barrett.** 1998. Repression of the telomerase catalytic subunit by a gene on human chromosome 3 that induces cellular senescence. Mol. Carcinog. 22:65–72.
21. **Horrigan, S. K., et al.** 2000. Delineation of a minimal interval and identification of 9 candidates for a tumor suppressor gene in malignant myeloid disorders on 5q31. Blood 95:2372–2377.
22. **Johnstone, R., et al.** 2001. Functional analysis of the leukemia protein ELL: evidence for a role in the regulation of cell growth and survival. Mol. Cell. Biol. 21:1672–1681.
23. **Kolfschoten, I., et al.** 2005. A genetic screen identifies PITX1 as a suppressor of RAS activity and tumorigenicity. Cell 121:849–858.
24. **Kugoh, H., K. Shigenami, K. Funaki, J. Barrett, and M. Oshimura.** 2003. Human chromosome 5 carries a putative telomerase repressor gene. Genes Chromosomes Cancer 36:37–47.
25. **Kuroiwa, Y., et al.** 1998. Efficient modification of a human chromosome by telomere-directed truncation in high homologous recombination-proficient chicken DT40 cells. Nucleic Acids Res. 26:3447–3448.
26. **Lamonerie, T., et al.** 1996. Ptx1, a bicoid-related homeo box transcription factor involved in transcription of the pro-opiomelanocortin gene. Genes Dev. 10:1284–1295.
27. **Lanctôt, C., A. Moreau, M. Chamberland, M. Tremblay, and J. Drouin.** 1999. Hindlimb patterning and mandible development require the Ptx1 gene. Development 126:1805–1810.
28. **Lin, S., and S. Elledge.** 2003. Multiple tumor suppressor pathways negatively regulate telomerase. Cell 113:881–889.
29. **Liu, D., and P. Lobie.** 2007. Transcriptional activation of p53 by Pitx1. Cell Death Differ. 14:1893–1907.
30. **Lord, R., et al.** 2005. Increased CDX2 and decreased PITX1 homeobox gene expression in Barrett's esophagus and Barrett's-associated adenocarcinoma. Surgery 138:924–931.
31. **Meaburn, K. J., C. N. Parris, and J. M. Bridger.** 2005. The manipulation of chromosomes by mankind: the uses of microcell-mediated chromosome transfer. Chromosoma 114:263–274.
32. **Nishimoto, A., et al.** 2001. Functional evidence for a telomerase repressor gene on human chromosome 10p15.1. Oncogene 20:828–835.
33. **Nozawa, K., K. Machara, and K. Isobe.** 2001. Mechanism for the reduction of telomerase expression during muscle cell differentiation. J. Biol. Chem. 276:22016–22023.
34. **Oh, S., Y. Song, J. Yim, and T. Kim.** 2000. Identification of Mad as a repressor of the human telomerase (hTERT) gene. Oncogene 19:1485–1490.
35. **Oh, S., Y. Song, J. Yim, and T. Kim.** 1999. The Wilms' tumor 1 tumor suppressor gene represses transcription of the human telomerase reverse transcriptase gene. J. Biol. Chem. 274:37473–37478.
36. **Ohmura, H., et al.** 1995. Restoration of cellular senescence program and repression of telomerase by human chromosome 3. Jpn. J. Cancer Res. 86:899–904.

37. **Oshimura, M., and J. C. Barrett.** 1997. Multiple pathways to cellular senescence: role of telomerase repressors. Eur. J. Cancer **33**:710–715.
38. **Peralta, R. C., et al.** 1998. Distinct regions of frequent loss of heterozygosity of chromosome 5p and 5q in human esophageal cancer. Int. J. Cancer. **78**:600–605.
39. **Qi, D. L., T. Ohhira, M. Oshimura, and H. Kugoh.** 2010. Human chromosome 5 carries a transcriptional regulator of human telomerase reverse transcriptase (hTERT). Biochem. Biophys. Res. Commun. **398**:695–701.
40. **Ramaswamy, S., et al.** 2001. Multiclass cancer diagnosis using tumor gene expression signatures. Proc. Natl. Acad. Sci. U. S. A. **98**:15149–15154.
41. **Renaud, S., D. Loukinov, F. Bosman, V. Lobanenkov, and J. Benhattar.** 2005. CTCF binds the proximal exonic region of hTERT and inhibits its transcription. Nucleic Acids Res. **33**:6850–6860.
42. **Rhodes, D., et al.** 2007. Oncomine 3.0: genes, pathways, and networks in a collection of 18,000 cancer gene expression profiles. Neoplasia **9**:166–180.
43. **Ritz, J., et al.** 2005. A novel transgenic mouse model reveals humanlike regulation of an 8-kbp human TERT gene promoter fragment in normal and tumor tissues. Cancer Res. **65**:1187–1196.
44. **Shang, J., X. Li, H. Ring, D. Clayton, and U. Francke.** 1997. Backfoot, a novel homeobox gene, maps to human chromosome 5 (BFT) and mouse chromosome 13 (Bft). Genomics **40**:108–113.
45. **Shang, J., Y. Luo, and D. Clayton.** 1997. Backfoot is a novel homeobox gene expressed in the mesenchyme of developing hind limb. Dev. Dyn. **209**:242–253.
46. **Singh, D., et al.** 2002. Gene expression correlates of clinical prostate cancer behavior. Cancer Cell **1**:203–209.
47. **Steenbergen, R. D., et al.** 2001. Telomerase suppression by chromosome 6 in a human papillomavirus type 16-immortalized keratinocyte cell line and in a cervical cancer cell line. J. Natl. Cancer Inst. **93**:865–872.
48. **Stewart, S., et al.** 2002. Telomerase contributes to tumorigenesis by a telomere length-independent mechanism. Proc. Natl. Acad. Sci. U. S. A. **99**: 12606–12611.
49. **Takakura, M., S. Kyo, M. Inoue, W. Wright, and J. Shay.** 2005. Function of AP-1 in transcription of the telomerase reverse transcriptase gene (TERT) in human and mouse cells. Mol. Cell. Biol. **25**:8037–8043.
50. **Tan, M., Y. Wang, K. Guan, and Y. Sun.** 2000. PTGF-beta, a type beta transforming growth factor (TGF-beta) superfamily member, is a p53 target gene that inhibits tumor cell growth via TGF-beta signaling pathway. Proc. Natl. Acad. Sci. U. S. A. **97**:109–114.
51. **Tanaka, H., et al.** 1998. Evidence for a putative telomerase repressor gene in the 3p14.2-p21.1 region. Genes Chromosomes Cancer **23**:123–133.
52. **Wang, S., Y. Zhao, C. Hu, and J. Zhu.** 2009. Differential repression of human and mouse TERT genes during cell differentiation. Nucleic Acids Res. **37**: 2618–2629.
53. **Won, J., J. Yim, and T. Kim.** 2002. Sp1 and Sp3 recruit histone deacetylase to repress transcription of human telomerase reverse transcriptase (hTERT) promoter in normal human somatic cells. J. Biol. Chem. **277**:38230–38238.
54. **Xiong, J., et al.** 2003. BRCA1 inhibition of telomerase activity in cultured cells. Mol. Cell. Biol. **23**:8668–8690.
55. **Xu, H. J., et al.** 1997. Reexpression of the retinoblastoma protein in tumor cells induces senescence and telomerase inhibition. Oncogene **15**:2589–2596.
56. **Yang, H., S. Kyo, M. Takatura, and L. Sun.** 2001. Autocrine transforming growth factor beta suppresses telomerase activity and transcription of human telomerase reverse transcriptase in human cancer cells. Cell Growth Differ. **12**:119–127.
57. **Zhang, Y., et al.** 2009. TGFBI deficiency predisposes mice to spontaneous tumor development. Cancer Res. **69**:37–44.

Gene Therapy (2012) 19, 34–48

www.nature.com/gt

ORIGINAL ARTICLE

In vivo delivery of *interferon-α* gene enhances tumor immunity and suppresses immunotolerance in reconstituted lymphopenic hosts

K Narumi[1,4], T Udagawa[1], A Kondoh[1], A Kobayashi[1], H Hara[1], Y Ikarashi[1], S Ohnami[2], F Takeshita[3], T Ochiya[3], T Okada[4], M Yamagishi[4], T Yoshida[2] and K Aoki[1]

T cells recognize tumor-associated antigens under the condition of lymphopenia-induced homeostatic proliferation (HP); however, HP-driven antitumor responses gradually decay in association with tumor growth. Type I interferon (IFN) has important roles in regulating the innate and adaptive immune system. In this study we examined whether a tumor-specific immune response induced by IFN-α could enhance and sustain HP-induced antitumor immunity. An intratumoral *IFN-α* gene transfer resulted in marked tumor suppression when administered in the early period of syngeneic hematopoietic stem cell transplantation (synHSCT), and was evident even in distant tumors that were not transduced with the IFN-α vector. The intratumoral delivery of the *IFN-α* gene promoted the maturation of CD11c$^+$ cells in the tumors and effectively augmented the antigen-presentation capacity of the cells. An analysis of the cytokine profile showed that the CD11c$^+$ cells in the treated tumors secreted a large amount of immune-stimulatory cytokines including interleukin (IL)-6. The CD11c$^+$ cells rescued effector T-cell proliferation from regulatory T-cell-mediated suppression, and IL-6 may have a dominant role in this phenomenon. The intratumoral *IFN-α* gene transfer creates an environment strongly supporting the enhancement of antitumor immunity in reconstituted lymphopenic recipients through the induction of tumor-specific immunity and suppression of immunotolerance.
Gene Therapy (2012) **19**, 34–48; doi:10.1038/gt.2011.73; published online 26 May 2011

Keywords: IFN-α; gene transfer; hematopoietic stem cell transplantation; IL-6; regulatory T cells

INTRODUCTION

The development of effective cancer immunotherapy is often difficult because cancer generates an immunotolerant microenvironment against the host immune system.[1] The central objective of cancer immunotherapy is to induce and sustain a tumor-specific immune response; that is, an *in vivo* generation of a large number of highly reactive antitumor lymphocytes that are not restrained by cancer-induced tolerance mechanisms.

It is known that lymphopenia is followed by spontaneous expansion of the remaining T cells in the periphery to restore the original T-cell pool size and maintain homeostasis.[2] Lymphopenia-induced homeostatic proliferation (HP) of T cells following autologous hematopoietic stem cell transplantation (HSCT) is driven by the recognition of self-antigens, and there is an opportunity to skew the T-cell repertoire during the T-cell recovery by engaging tumor-associated antigens (TAAs), leading to a break in tolerance developed by tumors.[2] In fact, a variety of animal tumor models showed that lymphopenic conditions are able to create an environment to mount an efficient antitumor immunity through an HP-induced expansion of T cells.[3–6] However, integration of other immunotherapeutic strategies is necessary to successfully eradicate pre-existing malignant tumors, because HP-driven antitumor responses decay gradually, as they are vulnerable to a development of tolerance.[5,6]

The interferon (IFN)-α protein is a pleiotropic cytokine regulating anti-proliferation, induction of cell death, anti-angiogenesis and immunomodulation, and has been used for treatment in a variety of cancers such as chronic myeloid leukemia, melanoma and renal cancer.[7,8] Although IFN-α was long thought to function mainly by suppressing tumor cell proliferation *in vivo*, more recently it has been established that type I IFNs have important roles in regulating the innate and adaptive arms of the immune system: upregulation of major histocompatibility complex class I gene, promotion of the priming and survival of T cells, enhancement of humoral immunity, increase of the cytotoxic activity of natural killer (NK) cells and CD8$^+$ T cells and activation of dendritic cells (DCs).[9,10] We also reported that in addition to the direct cytotoxicity in the injected site, intratumoral *IFN-α* gene transfer elicits a systemic tumor-specific immunity in several animal models.[11,12] Furthermore, our data showed that, because of the effective induction of antitumor immunity and the lower toxicity, an intratumoral route of the IFN vector is superior to an intravenous administration.[13]

In this study, we examined whether HP-induced antitumor activity can be enhanced by IFN-α gene transfer during a physiological

[1]Division of Gene and Immune Medicine, National Cancer Center Research Institute, Tokyo, Japan; [2]Division of Genetics, National Cancer Center Research Institute, Tokyo, Japan; [3]Division of Molecular and Cellular Medicine, National Cancer Center Research Institute, Tokyo, Japan and [4]Department of Internal Medicine, Kanazawa University Graduate School of Medical Science, Ishikawa, Japan
Correspondence: Dr K Aoki, Section for Studies on Host-Immune Response, National Cancer Center Research Institute, 5-1-1 Tsukiji, Chuo-ku, Tokyo 104-0045, Japan.
E-mail: kaoki@ncc.go.jp
Received 25 September 2010; revised 4 April 2011; accepted 19 April 2011; published online 26 May 2011

immune reconstitution, and investigated mechanisms of the enhancement. From the viewpoint of IFN-α immune therapy also, an autologous HSCT following a preconditioning is expected to introduce a fresh immune system, in which tolerance to tumor cells is not yet induced, and may present a unique opportunity for IFN-α to augment efficacy of the immune therapy.

RESULTS

Adenovirus-mediated *IFN-α* gene transfer induces significant antitumor effect with synHSCT

To examine whether HP of T cells could induce antitumor immunity in lymphopenic hosts, BALB/c mice were injected subcutaneously with CT26 colon cancer cells shortly after lethal (9 Gy) irradiation, and then bone marrow and T cells were infused into the mice. Tumor growth was significantly suppressed in the syngeneic HSCT (synHSCT) recipients (Figure 1a) as previously reported.[6] HSCT with immunodeficient mice did not show the tumor growth suppression as compared with non-transplanted mice (data not shown), indicating that the antitumor effect is not mediated by a nonspecific effect of irradiation or lymphocyte infusion. Then, to examine whether a combination of intratumoral *IFN-α* gene transfer enhances the antitumor effect of synHSCT, 5×10^6 PFU (plaque forming unit) of Ad-mIFN was injected once into the tumor at 5 days after the CT26 inoculation. To detect a synergistic effect, we used a low dose (5×10^6 PFU) of Ad-mIFN in this experiment, although the antitumor effect of intratumoral Ad-mIFN injection is dose-dependent, and a strong antitumor effect is induced by a high dose ($5–10\times10^7$ PFU) of Ad-mIFN alone.[12,13] Although the low dose of Ad-mIFN alone suppressed tumor growth only slightly in naïve mice as expected, a significant growth suppression was observed in the synHSCT recipients compared with the injection of a control Ad-AP (Figure 1b).

Injection of IFN-α-expressing plasmid suppresses tumor growth in synHSCT recipients

We observed a significant growth suppression of colon cancer in a lymphopenic host by an injection of a low dose of Ad-mIFN (Figure 1b). Although the *in vivo* gene transduction efficiency of the plasmid vector is lower than that of the virus vector, the lipofection/

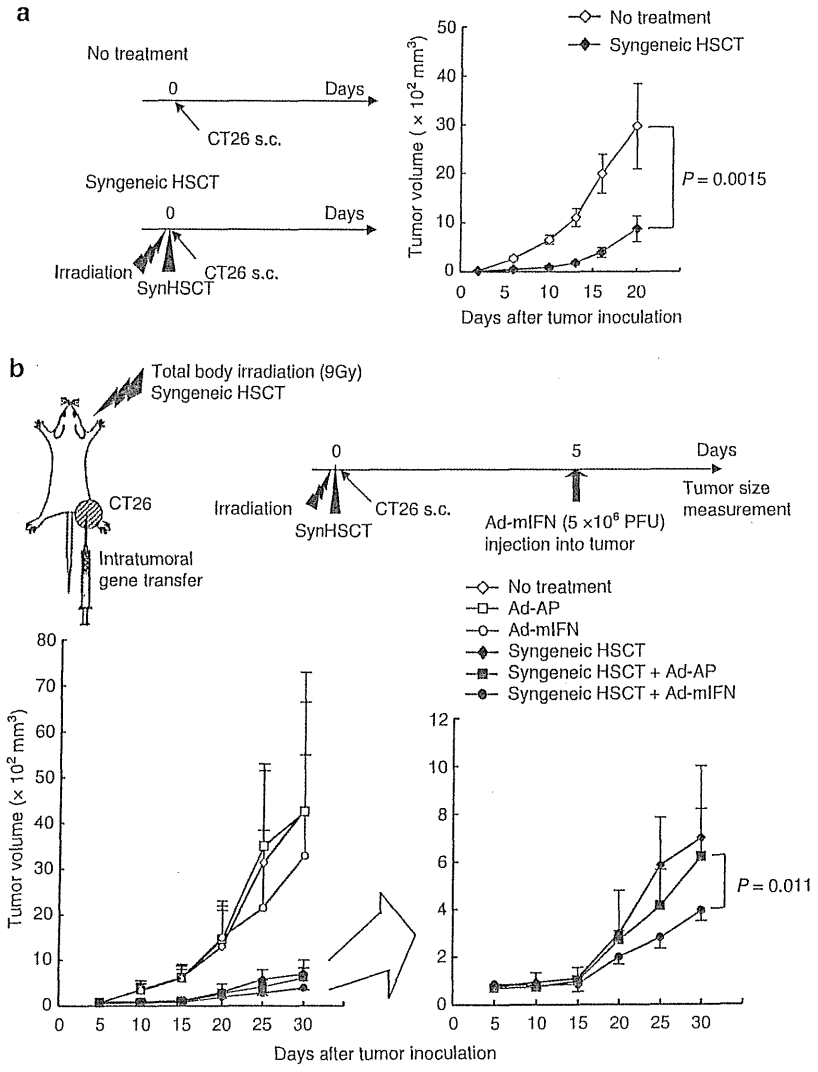

Figure 1 Adenovirus-mediated *IFN-α* gene transfer enhances antitumor effect in synHSCT recipients. (**a**) Growth suppression of subcutaneous tumors in the synHSCT mice. The mice received a lethal dose (9 Gy) of irradiation, followed by a transfusion of bone marrow and splenic T cells, and then CT26 cells were inoculated into right legs. As a control, CT26 cells were inoculated in non-irradiated mice (n=7). (**b**) A combination of syngeneic HSCT and IFN-α adenovirus injection. When CT26 subcutaneous tumors were established, 5×10^6 PFU of Ad-mIFN or control vector (Ad-AP) were injected once into the tumors (n=6–8). The experiments were repeated two times.

polyfection of the plasmid vector has an excellent safety profile.[14] Therefore, we examined whether tumor growth suppression would be observed by an injection of an IFN-α-expressing plasmid (pIFN-α). First, we confirmed that CT26 and Renca cells transfected with the pIFN-α produced significant amounts of IFN-α protein in the culture medium (Figure 2a), and showed growth suppression *in vitro* (Figure 2b). In CT26 tumor-bearing BALB/c mice, the injection of pIFN-α complexed with cationic liposome (DMRIE-DOPE) expressed IFN-α in the tumors in a dose-dependent manner, and an IFN-α concentration by the injections of pIFN-α (30 μg, three times) was comparable with that of Ad-mIFN (5×10^6 PFU, once) (Figure 2c). The plasmid-mediated IFN-α expression continued for more than 10 days after gene transfer and returned to a control level at 14 days after gene transfer (Figure 2d).

Then, to examine the *in vivo* antitumor effect of a plasmid-mediated *IFN-α* gene transfer, a pIFN-α/liposome complex was injected into the CT26 subcutaneous tumors at 7 days after the transplantation. The injection of pIFN-α slightly suppressed tumor growth compared with the non-injected control group, whereas the tumor-suppressive effect by the injection of pIFN-α was significantly enhanced in the lymphopenic mice that received synHSCT (Figure 2e). The results suggested that an *in vivo* injection of pIFN-α induced antitumor immunity in lymphopenic hosts as effectively as the Ad-mIFN. Regarding the timing of intratumoral *IFN-α* gene transfer, the injection of pIFN-α at 8 weeks after transplantation did not enhance the antitumor immunity, whereas a substantial antitumor effect was observed by *IFN-α* gene transfer in the earlier period (2–6 weeks) after the transplantation (Figure 2f), suggesting that intratumoral *IFN-α* gene transfer during immune reconstitution can induce a synergistic antitumor effect. In the mice treated with *IFN-α* gene transfer at 6 weeks after HSCT, tumor growth suppression was still recognized ($P=0.016$) at day 42 and the survival of the treated mice was significantly prolonged as compared with the injection of the control plasmid (Figure 2g). All treated mice looked healthy during the course of the experiments, and the blood chemistry (albumin, alanine transaminase, total bilirubin, alkaline phosphatase, blood urea nitrogen, creatinine) showed no abnormal values in the treated mice at 5 weeks after the HSCT.

Intratumoral *IFN-α* gene transfer increases tumor-infiltrating lymphocytes after synHSCT

It is known that a large number of tumor-infiltrating lymphocytes (TILs) results in a better prognosis for cancer patients.[15] To examine whether an increase of TILs in treated tumors is related to tumor growth suppression, immunohistochemical staining of CD4 and CD8-positive cells was performed at 1–4 weeks after synHSCT. In this experiment, CT26 cells were inoculated on legs at 1 week before synHSCT, and the number of $CD4^+$ and $CD8^+$ T cells infiltrated into the tumors was examined at the day of synHSCT to evaluate how the number of immune cells increases in the tumors by the combination therapy as compared with the pre-treatment status. In this established tumor model also, a significant antitumor effect was recognized in the synHSCT mice with the *IFN-α* gene transfer (Figure 3a).

The numbers of $CD4^+$ and $CD8^+$ cells gradually diminished in the non-treated tumors, whereas the TILs increased in the tumors of synHSCT mice. Intratumoral *IFN-α* gene transfer further increased the numbers of TILs significantly in synHSCT recipients at 4 weeks (Figure 3b), suggesting that intratumoral *IFN-α* gene transfer enhances and prolongs HP-induced antitumor immunity after synHSCT.

Then, to examine the cytotoxic activity of TILs, $CD8^+$ T cells were isolated from tumors in the treated mice. The flow cytometry showed that the expression of perforin on $CD8^+$ TILs was significantly enhanced in the synHSCT alone group and in the combination therapy-treated group, suggesting that synHSCT creates an environment to enhance the killing activity of TILs in the tumors (Figure 3c).

Tumor-specific lymphocytes are activated by intratumoral *IFN-α* gene transfer in synHSCT recipients

To examine the immune reaction to intratumoral *IFN-α* gene transfer in synHSCT recipients, splenocytes were extracted from the treated mice and cultured with CT26 cells. An enzyme-linked immunosorbent spot assay showed that the average number of IFN-γ-producing splenocytes in response to CT26 cells was slightly increased in the synHSCT alone group, whereas a combination of synHSCT and intratumoral *IFN-α* gene transfer further increased the IFN-γ-positive spots (Figure 4a, left panel). The numbers of the spots in splenocytes co-cultured with syngeneic lymphocytes were not changed in the treated groups (Figure 4a, right panel). To analyze the subset of activated lymphocytes, the frequency of tumor-reactive immune cells was determined by intracellular cytokine staining and flow cytometry. The percentage of $CD4^+$ and $CD8^+$ T cells stimulated to produce IFN-γ in response to CT26 cells increased significantly in the mice treated by a combination of synHSCT and intratumoral *IFN-α* gene transfer, and there was also an increase in the percentage of IFN-γ-positive NK cells (Figure 4b). The results indicated that the numbers of tumor-reactive lymphocytes were increased synergistically by a combination therapy.

An *in vitro* cytotoxic assay showed that the splenocytes derived from the synHSCT mice recognized and lysed CT26 cells, and *IFN-α* gene transfer enhanced the cytolysis to CT26 cells (Figure 4c, left panel). To

Figure 2 Plasmid vector-mediated *IFN-α* gene transfer induces a significant antitumor effect in synHSCT recipients. (**a**) *In vitro* IFN-α concentration in the medium of cancer cells transfected with pIFN-α. CT26 or Renca cells were transfected with pIFN-α, and 48 h later, IFN-α concentration in the culture medium was measured by enzyme-linked immunosorbent assay (ELISA; Immunotech, Marseille Cedex, France). pEGFP was used as a control. (**b**) *In vitro* cytotoxicity of pIFN-α transfection. The cell growth was determined by an *in vitro* cell proliferation assay at 5 days after transfection. The data are expressed as relative cell growth (OD_{450} of indicated cells/OD_{450} of untreated cells). Reagent; Lipofectamine 2000. (**c**) *In vivo* IFN-α concentration in the tumors transfected with pIFN-α. Various amounts (10–30 μg) of pIFN-α complexed with liposome were injected three times into the CT26 tumors at 7, 9 and 11 days after the tumor inoculation. Ad-mIFN (5×10^6 PFU) was injected once into the tumors at day 9. Tumors were collected at day 12, and the IFN-α concentration was measured by ELISA ($n=4$). (**d**) Time course of IFN-α expression in the tumors. The IFN-α levels were measured in the subcutaneous tumors during 14 days after intratumoral injection of pIFN-α (30 μg)/liposome complex at days 7, 9 and 11 ($n=4$–5). The statistical difference between IFN-α concentration in the indicated days and at day 7 is presented. (**e**) A combination of syngeneic HSCT and intratumoral *IFN-α* gene transfer caused marked tumor growth suppression. The pIFN-α (30 μg)/liposome complex was injected into the CT26 tumors at 7, 9 and 11 days after the tumor inoculation in the synHSCT mice ($n=7$). The experiments were repeated two times. (**f**) Intratumoral *IFN-α* gene transfer during an early phase of immune reconstitution enhances the antitumor effects. Syngeneic HSCTs to the BALB/c mice were staggered at intervals of 2 weeks, followed by a subcutaneous injection of CT26 cells and intratumoral *IFN-α* gene transfer at days 7, 9 and 11 ($n=6$–8). (**g**) Intratumoral *IFN-α* gene transfer significantly extends the survival of synHSCT mice ($n=7$). The pIFN-α/liposome complex was injected into the CT26 tumors at 6 weeks after the HSCT, and survival of the mice was compared with the mice injected with a control plasmid ($n=7$).

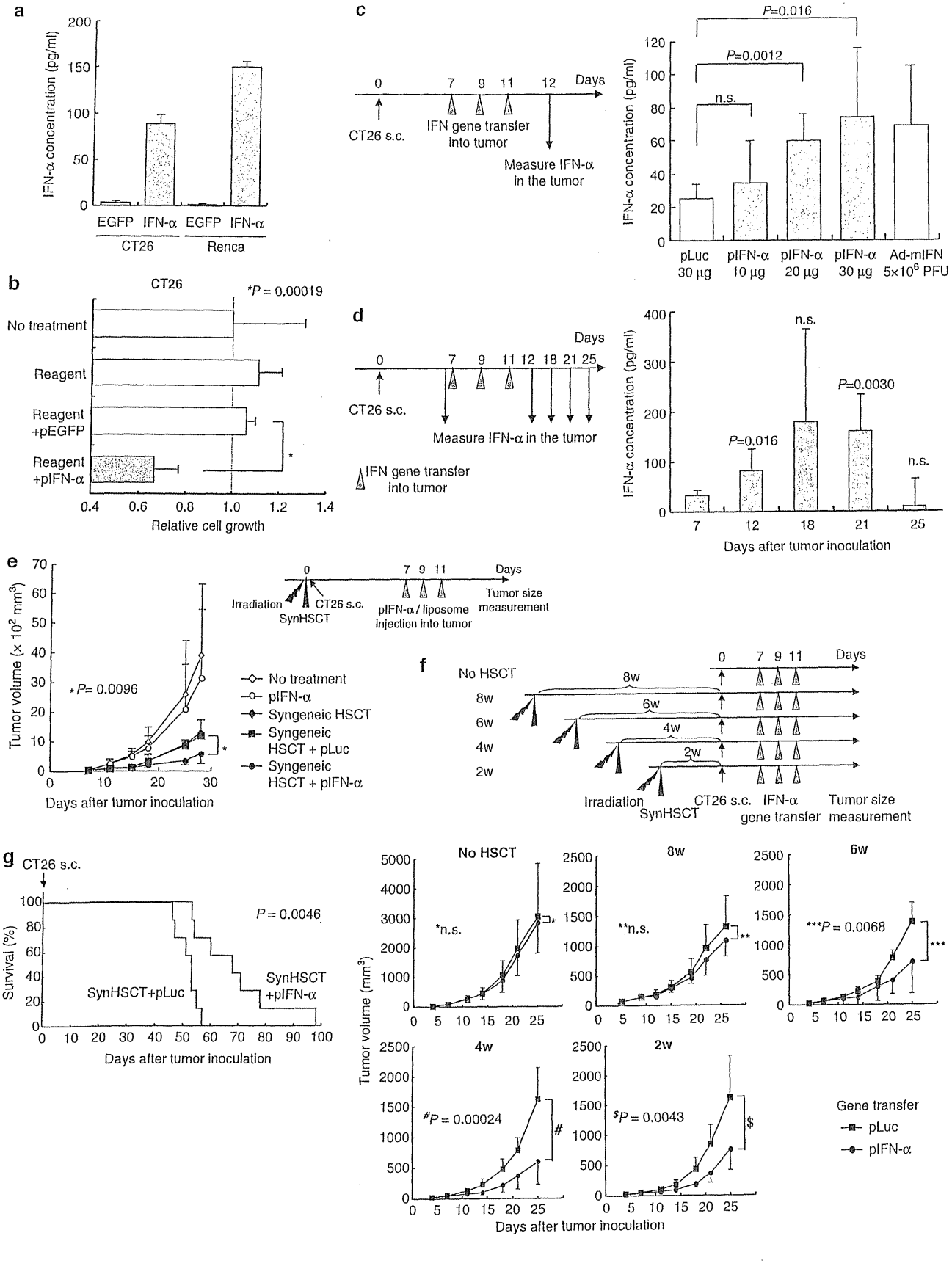
a
IFN-α concentration (pg/ml)
200
150
100
50
0
EGFP IFN-α EGFP IFN-α
CT26
Renca
b
CT26
*P = 0.00019
No treatment
Reagent
Reagent +pEGFP
Reagent +pIFN-α
0.4 0.6 0.8 1.0 1.2 1.4
Relative cell growth
c
0 7 9 11 12 Days
CT26 s.c.
IFN gene transfer into tumor
Measure IFN-α in the tumor
P=0.016
P=0.0012
n.s.
IFN-α concentration (pg/ml)
120
100
80
60
40
20
0
pLuc 30 μg
pIFN-α 10 μg
pIFN-α 20 μg
pIFN-α 30 μg
Ad-mIFN 5×10^6 PFU
d
0 7 9 11 12 18 21 25 Days
CT26 s.c.
Measure IFN-α in the tumor
IFN gene transfer into tumor
IFN-α concentration (pg/ml)
400
300
200
100
0
n.s.
P=0.016
P=0.0030
n.s.
7 12 18 21 25
Days after tumor inoculation
e
Tumor volume (× 10^2 mm^3)
70
60
50
40
30
20
10
0
*P= 0.0096
0 10 20 30
Days after tumor inoculation
0 7 9 11 Days
Irradiation
CT26 s.c.
SynHSCT
pIFN-α / liposome injection into tumor
Tumor size measurement
No treatment
pIFN-α
Syngeneic HSCT
Syngeneic HSCT + pLuc
Syngeneic HSCT + pIFN-α
f
No HSCT
8w
6w
4w
2w
0 7 9 11 Days
Irradiation
SynHSCT
CT26 s.c.
IFN-α gene transfer
Tumor size measurement
g
CT26 s.c.
Survival (%)
100
80
60
40
20
0
P = 0.0046
SynHSCT+pLuc
SynHSCT +pIFN-α
0 10 20 30 40 50 60 70 80 90 100
Days after tumor inoculation
No HSCT
*n.s.
8w
**n.s.
6w
***P = 0.0068
4w
#P = 0.00024
2w
$P = 0.0043
Tumor volume (mm^3)
5000
4000
3000
2000
1000
0
2500
2000
1500
1000
500
0
0 5 10 15 20 25
Days after tumor inoculation
Gene transfer
pLuc
pIFN-α

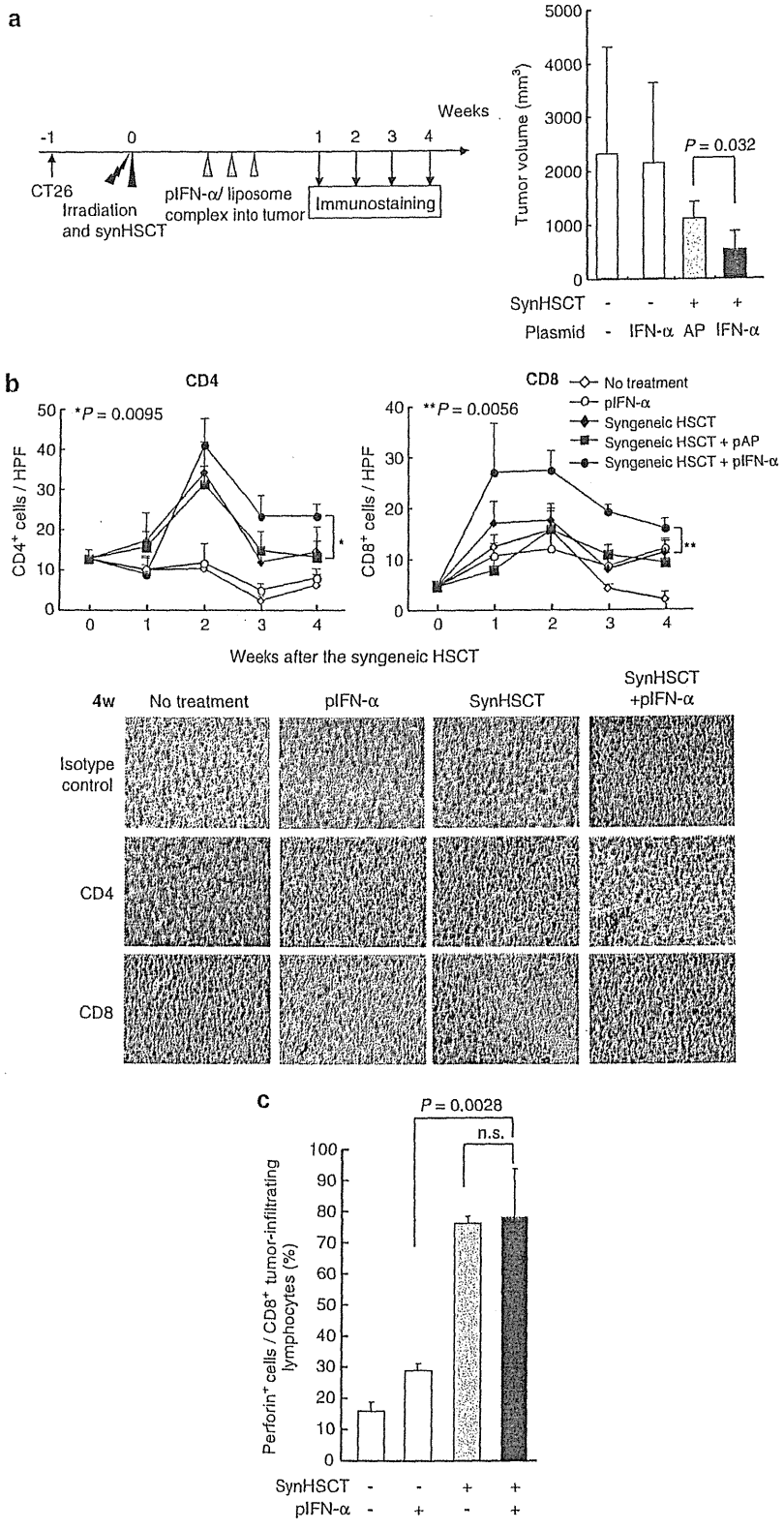

Figure 3 Immunostaining of treated tumors. (**a**) Antitumor effect of *IFN-α* gene transfer for established tumors in the synHSCT recipient mice. CT26 cells were inoculated on the right legs of BALB/c mice at 1 week before the synHSCT, and the pIFN-α/liposome complex was injected into CT26 tumors for three times. The tumor volumes at 3 weeks after the *IFN-α* gene transfer are presented. (**b**) Infiltration of immune cells in the tumors. The subcutaneous tumors were resected at the indicated days (n=3), and stained with CD4 and CD8 antibodies. The $CD4^+$ (upper left) and $CD8^+$ cells (upper right) were counted by microscopy in five high-power fields (×400). Representative photographs of stained cells at 4 weeks after the gene transfer are presented in the lower panel (×400). (**c**) Expression of perforin on $CD8^+$ tumor-infiltrating lymphocytes. The $CD8^+$ T cells were isolated from the tumors using mouse CD8 MicroBeads and AutoMACS magnetic sorter (Miltenyi Biotec, Bergisch Gladbach, Germany). The flow cytometry of perforin (eBioOMAK-D; eBioscience, San Diego, CA, USA) was performed on the $CD8^+$ TILs (n=3). The frequency of $perforin^+$ cells per $CD8^+$ cells is presented.

show the major histocompatibility complex class I-restriction of cytotoxicity, lymphocytes were pre-incubated with the anti-CD4 or anti-CD8 antibodies before the cytolysis for CT26 cells. The addition of anti-CD8 antibody markedly inhibited the cell lysis (Figure 4c, right panel).

To explore what kind of lymphocytes contribute to antitumor immunity *in vivo*, the mice were treated with anti-CD4, anti-CD8 and anti-asialo GM1 antibodies intraperitoneally to deplete $CD4^+$ T cells, $CD8^+$ T cells and NK cells, respectively. Depletion of all of the three populations canceled antitumor effect almost completely. Depletion of each $CD4^+$ T-cell, $CD8^+$ T-cell or NK cell showed some growth advantages but still resulted in significant tumor growth inhibition and, in particular, $CD8^+$ T cells appeared to contribute more strongly than $CD4^+$ T and NK cells (Figure 4d).

Intratumoral *IFN-α* gene transfer causes growth suppression in not only treated but also distant tumors

To evaluate the therapeutic efficacy of *IFN-α* gene transfer against tumors at distant sites in synHSCT recipients, the mice were inoculated with CT26 cells on both legs and Renca cells on the back, and an IFN-α plasmid/liposome complex was injected into the CT26 tumor on the right leg. The *IFN-α* gene transfer significantly suppressed the growth of not only the right leg CT26 tumors but also the left CT26 tumors that were not transfected with the *IFN-α* gene, whereas the growth of Renca tumors on the back was not influenced by the *IFN-α* gene transfer into the CT26 tumors (Figure 5a). When we exchanged CT26 and Renca cells, the antitumor effect was *vice versa* (Figure 5b). The results indicated that intratumoral *IFN-α* gene transfer enhances a vector-injected-tumor specific immunity systemically in the synHSCT recipients.

Liver metastasis is one of the most frequent causes of mortality in patients with gastrointestinal cancer such as colorectal cancer. As another model of distant metastasis, CT26-Luc cells were injected beneath the splenic capsule to generate liver metastasis, and CT26 cells were inoculated into the right leg. Intratumoral *IFN-α* gene transfer suppressed tumor growth of subcutaneous tumors on the legs (Figure 5c, upper left panel) as observed in Figure 2e, and the growth of abdominal tumors was also markedly suppressed, which were evaluated by photon counts on the IVIS imaging system (IVIS; Xenogen, Alameda, CA, USA), in the synHSCT mice (Figure 5c, upper right and lower panels). Twenty-one days after tumor inoculation, the mice were killed and the livers were examined by the IVIS imaging. Livers from non-treated mice showed many photon-positive spots, whereas livers from the mice treated by a combination therapy revealed a fewer number of photon-positive spots (Figure 5d, upper panel), which was confirmed by photon counts in those livers (Figure 5d, lower panel). These results indicated that a combination therapy is effective for preventing and regressing liver metastases.

A combination therapy enhances maturation of $CD11c^+$cells and their antigen presentation

To verify whether the intratumoral *IFN-α* gene expression promotes the maturation of DCs in the tumor, we isolated $CD11c^+$ cells from the regional lymph nodes of treated tumors. Flow cytometry showed that expressions of CD40, CD80, CD83 and CD86 were clearly upregulated by the *IFN-α* gene transfer (data not shown and see Narumi *et al.*[13]). Then, the expression of CD83 was examined in the $CD11c^+$ cells isolated from tumors. The frequency of $CD83^+$ cells was increased in IFN/HSCT-$CD11c^+$ cells compared with those in IFN-$CD11c^+$ and HSCT-$CD11c^+$ cells (Figure 6a, left panel), suggesting that IFN-α expression results in the maturation of $CD11c^+$ cells. Then, to examine the antigen-presentation capacity of the $CD11c^+$ cells in the tumors, the lymphocytes isolated from naïve mice were co-cultured with the $CD11c^+$ cells and mitomycin C-treated CT26 cells for 3 days. An enzyme-linked immunosorbent spot assay showed that the IFN/HSCT-$CD11c^+$ cells increased the number of IFN-γ-positive lymphocytes in response to CT26 cells (Figure 6a, middle panel). The production of IFN-γ from the $CD11c^+$ cells *per se* was minimal. Lymphocytes under HP are considered to be primed to TAAs. When lymphocytes isolated from tumor-bearing synHSCT mice were co-cultured with the $CD11c^+$ cells and mitomycin C-treated CT26 cells, the stimulation by IFN/HSCT-$CD11c^+$ cells resulted in a higher number of IFN-γ-secreting lymphocytes than those of IFN-$CD11c^+$ and HSCT-$CD11c^+$cells (Figure 6a, right panel). The results indicated that the antigen-presentation by $CD11c^+$ cells was enhanced by the IFN-α expression in the tumors in synHSCT mice.

$CD11c^+$cells treated by a combination therapy suppresses the activity of regulatory T cells

To analyze the cytokine expression profile of the $CD11c^+$ cells, we collected $CD11c^+$ cells from the treated tumor at 2 weeks after *IFN-α* gene transfer, cultured the cells *in vitro* for 48 h and measured the expression of various cytokines in the medium. The IFN/HSCT-$CD11c^+$ cells produced a large amount of immune-stimulatory cytokines such as interleukin (IL)-1β, IL-6 and IL-12 (Figure 6b), which may enhance the proliferation and activation of lymphocytes in the treated mice. Among the immunosuppressive cytokines (IL-4, IL-10 and transforming growth factor-β), IL-10 production is increased in IFN/HSCT-$CD11c^+$ cells. The enhanced IL-12 production might promote the production of IL-10 in some population of the $CD11c^+$ cells as a negative feedback mechanism.[16] However, the large amount of immune-stimulatory cytokines may overcome the suppressive effect of IL-10 in the tumors treated with the combination therapy.

IL-6 is of particular interest, because, when released from DCs, it is critical for overcoming Tregs-mediated immune suppression.[17] When the $CD11c^+$ cells isolated from the spleen of synHSCT and non-HSCT mice were cultured in the medium containing IFN-α protein, the cells produced IL-6 in a dose-response manner (Figure 7a). To examine whether the $CD11c^+$ cells inhibit the suppressive activity of Tregs, $CD11c^+$ cells were isolated from regional lymph nodes and co-cultured with $CD4^+CD25^-$ T cells (target) and $CD4^+CD25^+$ Tregs in mouse anti-CD3 T-cell activation plates. When Tregs were co-cultured with the control $CD11c^+$ cells isolated from non-treated mice, Tregs effectively suppressed the proliferation of target T cells. The co-culture with IFN/HSCT-$CD11c^+$ cells canceled the suppressive activity of Tregs for effector T cells (Figure 7b). The supernatant of IFN/HSCT-$CD11c^+$ cells also inhibited the suppressive activity of Tregs, and the addition of anti-IL-6 antibody in the medium restored the activity of Tregs, indicating that the critical factor of $CD11c^+$ cell-mediated inhibition of Tregs is IL-6, produced from activated $CD11c^+$ cells (Figure 7c).

Then, to examine the *in vivo* effect of intratumoral IFN-α expression on Tregs, we collected lymphocytes from treated tumors in synHSCT mice. Flow cytometry showed that intratumoral *IFN-α* gene transfer decreased the ratio of $Foxp3^+$ cells per $CD4^+$ T cells in the tumors of synHSCT mice, whereas the ratio of $Foxp3^+$ cells in the spleen was same as that in the non-treated mice (Figure 7d). The results suggested that IL-6 produced from $CD11c^+$ cells decreases the ratio of Tregs in the treated tumors. IFN-α expression may result in the extensive infiltration of T cells into the tumors of synHSCT mice (Figure 3b), and the number of $Foxp3^+$ cells also might increase in the